

TALLINN UNIVERSITY OF TECHNOLOGY
School of Information Technologies

Emmanuel Chimaobi Nelson 184607IVEM

**SYNCHRONOUS MEASUREMENT OF LOW-
LEVEL HIGH-FREQUENCY CURRENT
USING A TRANSFORMER**

Master's thesis

Supervisor: Jaan Ojarand
PhD

Co-supervisor: Kaiser Pärnamets
Lecturer

Tallinn 2020

TALLINNA TEHNIKAÜLIKOOL
Infotehnoloogia teaduskond

Emmanuel Chimaobi Nelson 184607IVEM

KÕRGSAGEDUSLIKU NÕRKVOOLU SÜNKROONMÕÕTMINE TRAFIO ABIL

Magistritöö

Juhendaja: Jaan Ojarand

PhD

Kaasjuhendaja: Kaiser Pärnamets

Lektor

Tallinn 2020

Author's declaration of originality

I hereby certify that I am the sole author of this thesis. All the used materials, references to the literature and the work of others have been referred to. This thesis has not been presented for examination anywhere else.

Author: Emmanuel Chimaobi Nelson

18.05.2020

Abstract

Current measurements are an important part of electrical/electronic research. The current measurement may also be required in control systems and protection circuits. Current measurement solutions can be divided into contact measurement and contactless measurement. The contactless measurement may be required for galvanic isolation of circuits, but also in applications where the effect of properties of contacts (electrodes) on the measurement results is not desirable, such as impedance spectroscopy of liquids, which is one potential application of the present research. The thesis deals with the synchronous measurement of high-frequency weak current using an isolating transformer, where the current range is from nano amperes to milliamperes, and the frequency range is 10 kHz to 5 MHz. The introductory part describes various current measurement solutions. It compares their features, including, for example, current measurement with a series resistor, a Hall effect sensor, a Fluxgate sensor, a Rogowski coil, and a current transformer. At lower values of the measured current, the signal-to-noise ratio becomes the main limiting factor for the accuracy and resolution of the measurements. In order to obtain a better signal-to-noise ratio, it is necessary to find the optimal parameters of the transformer, with smaller dimensions also being preferred. Since one potential application is impedance spectroscopy, the best result is obtained when the excitation signal (in this case, the measured current) and the response signal (in this case, the transformer secondary voltage) is measured in synchronous mode. The advantage of synchronous measurement is the possibility to use an output filter with a narrow frequency band, which allows to effectively suppress interference at adjacent frequencies, thus ensuring a good signal-to-noise ratio. The thesis compares and analyses the measurement results obtained with different transformers and presents recommendations for better results.

Keywords: Current measurement, Contactless measurement, Current transformer, Synchronous measurement

This thesis is written in English and is 38 pages long, including 5 chapters, 37 figures and 2 tables.

Annotatsioon

Voolu mõõtmised on elektriliste / elektrooniliste uuringute oluline osa. Voolu mõõtmist võib vaja minna ka juhtimissüsteemides ja kaitseskeemides. Voolu mõõtmise lahendused võib jagada kontakt-mõõtmiseks ja kontaktivabaks mõõtmiseks. Kontaktivaba mõõtmist võib vaja minna ahelate galvaaniliseks isoleerimiseks, kuid ka rakendustes, kus kontaktide omaduste mõju mõõtetulemustele ei ole soovitatav, näiteks vedelike impedants-spektroskoopia, mis on käesoleva uurimistöo üheks potentsiaalseks rakenduseks. Lõputöös käsitletakse kõrgsagedusliku nõrkvoolu sünkroonmõõtmist eraldustrafo abil, kus voolude piirkond on nanoampriitest milliampriteni ja sagedusvahemik 10 kHz kuni 5 MHz. Sissejuhatavas osas kirjeldatakse erinevaid voolu mõõtmise lahendusi ja võrreldakse nende omadusi, sealhulgas näiteks voolu mõõtmine järjestiktakisti abil, Halli efektil põhineva anduriga, „Fluxgate“ anduriga, Rogowski pooliga ja voolutrafoga.

Mõõdetava voolu väiksemate väärtuste korral muutub signaal-müra suhe peamiseks mõõtmiste täpsust ja resolutsiooni piiravaks teguriks. Parema signaal-müra suhte saamiseks on vaja leida trafo optimaalsed parameetrid, kusjuures on eelistatud on ka väiksemad mõõtmised. Kuna üheks potentsiaalseks rakenduseks on impedants-spektroskoopia, saadakse parim tulemus siis, kui ergutussignaali (antud juhul mõõdetav vool) ja vastussignaali (antud juhul trafo sekundaarpinge), mõõdetakse sünkroonrežiimis. Sünkroonmõõtmine eeliseks on kitsa sagedusribaga väljundfiltri kasutamise võimalus, mis võimaldab efektiivselt maha suruda kõrval-sagedustel esinevad häired, tagades nii hea signaal-müra suhte.

Töös on võrreldud ja analüüsitud erinevate trafodega saadud mõõtetulemusi ja esitatud soovitusid paremate tulemuste saamiseks.

Märksõnad: Voolu mõõtmine, kontaktivaba mõõtmine, voolutrafo, sünkroonmõõtmine

Lõputöö on kirjutatud Inglise keeles ning sisaldab teksti 38 leheküljel, 5 peatükki, 37 joonist, 2 tabelit.

Acknowledgement

Firstly, I thank God Almighty for his grace, mercy and provision in my life. I thank him for the strength he gave me throughout my master's program.

I am deeply indebted to my supervisor, senior research scientist Jaan Ojarand, who supported me through my thesis with his objective supervision, constructive criticism, valuable suggestions open-mindedness and abundant knowledge in this field.

I offer my sincere gratitude to my co-supervisor, lecturer Kaiser Pärnamets, who helped me a lot during the documentation of this thesis with his experience.

I give thanks to my program director, lecturer Andres Eek, whose inspiring suggestions and encouragement helped me throughout this thesis. He provided inspiration, and support from the onset of this thesis, without which my studies couldn't have been completed.

Furthermore, my gratitude goes to the School of Information Technology for their organization and financially support throughout my program.

Finally, to all my professors and colleagues who has helped me in one way or the other during this program. I will really miss you all, but I will always remember you.

Dedication

I dedicate this thesis to my late parents Elder Nelson Chimezie Akanazu and Deaconess Cordelia Akanazu. They taught me to persist and equipped me to face challenges with confidence and humility. They were source of inspiration, encouragement and support. What they instilled in me has been a driving force in my life endeavours. Though they are not here anymore, their presence will always be felt in my life.

List of abbreviations and terms

AC	Alternating Current
ADC	Analog to Digital Converter
AM	Amplitude Modulation
AMP	Amplifier
B	Magnetic field
CT	Current Transformer
DAC	Digital to Analog Converter
DC	Direct Current
EMF	Electromotive force
FG	Fluxgate
FM	Frequency Modulation
IA	Impedance Analyzer
L	Inductor
MF	Medium Frequency
MFLI	Medium Frequency Lock-In Amplifier
PC	Personal Computer
RMS	Root Mean Square
SNR	Signal to Noise Ratio
STD	Standard Deviation
USB	Universal Serial Bus
WWW	World Wide Web
Φ	Magnetic flux

Table of contents

1 Introduction	14
1.1 Problem statement	14
1.2 Frequency, amplitude and RMS (<i>Root Mean Square</i>) value.....	15
1.3 Electromagnetic induction.....	15
1.4 Synchronous Measurement.....	16
2 Current Sensing Techniques.....	18
2.1 Current sensing based on Ohm’s Law of Resistance	18
2.1.1 Shunt Resistor.....	18
2.2 Current sensing based on Faraday’s Law of Induction	19
2.2.1 Rogowski coil current sensors.....	19
2.2.2 Current sensing using a Current Transformer	20
2.3 Current sensing by means of Magnetic Field Sensors.....	21
2.3.1 Hall Effect	21
2.3.2 Fluxgate Sensing	22
2.4 Comparison of the Current Sensors.....	24
3 Transformer	25
3.1 Transformers.....	25
3.2 Working Principles of a Transformer	26
3.3 EMF Equation of Transformer:	27
3.4 Transformer Turns ratio:	27
3.5 Components of a Transformer	28
3.5.1 Transformer Core used	28
3.5.2 Inductor.....	29
4 Measurement Setup and Results.....	30
4.1 Introduction of MFLI Lock-in Amplifier	30
4.1.1 Lock-in Amplifier working principle	30
4.1.2 Summary of MFLI Lock-in Amplifier	31
4.1.3 Description of MFLI Lock-in Amplifier	31

4.2 Measurement setup	31
4.3 Procedure	32
4.3.1 Impedance data of secondary turns	33
4.4 Results and Analysis.....	34
4.4.1 Introduction to the current measurement with a transformer	34
4.4.2 The frequency response	36
4.4.3 Comparison of the frequency response of V_{in} and STD with different cores and number of turns	41
4.4.4 The influence of the series resistance on the primary side of the transformer	42
4.4.5 Measurement errors.	45
4.5 Conclusion based on Measurement results.....	49
5 Summary and Recommendations	50
References	52

List of figures

Figure 1. Voltage versus Time	15
Figure 2. Shunt Resistor current sensing	19
Figure 3. Rogowski coil current sensing	20
Figure 4. Current Transformer current sensing	21
Figure 5. Hall Effect current sensing	22
Figure 6. Fluxgate current sensing	23
Figure 7. Single Phase Transformer Schematic [17]	25
Figure 8. Simplified equivalent Circuit of a Transformer [1]	26
Figure 9. Simplified equivalent circuit of a real transformer [1]	26
Figure 10. Cores with secondary windings	28
Figure 11.(a) series resistor, and (b) measurement setup	32
Figure 12. Simplified measurement circuit	32
Figure 13. Impedance magnitude (a) and Phase (b) with 10 turns for T50-26 core.....	33
Figure 14. Impedance magnitude (a) and Phase (b) with 30 turns for T50-26 core.....	33
Figure 15. Impedance magnitude (a) and Phase (b) with 100 turns for T50-26 core.....	34
Figure 16. Impedance magnitude (a) and Phase (b) with 10 turns ELP 18 PC200 core	34
Figure 17. Equivalent circuit of the measurement setup	36
Figure 18. Modelled frequency response of the V_{in} (a) and corresponding phase response (b)	36
Figure 19. The measured frequency response of the V_{in} (a) and corresponding phase response (b)	37
Figure 20. The frequency response of the V_{in} at measured RMS (<i>Root mean Square</i>) currents from 1 nA to 1 mA (a) and corresponding relative STD (<i>Standard Deviation</i>) (b) with R_{load} 100 k Ω	39
Figure 21. The frequency response of the V_{in} at measured RMS currents from 1 nA to 1 mA (a) and corresponding relative STD (b) with R_{load} 100 Ω	39
Figure 22. The frequency response of the V_{in} at measured RMS currents from 1 nA to 1 mA (a) and corresponding relative STD (b) with R_{load} 1k Ω	40

Figure 23. The frequency response of the V_{in} at measured RMS currents from 10 nA to 5 mA (a) and corresponding relative STD (b).....	41
Figure 24. The frequency response of the V_{in} at measured RMS currents from 10 nA to 5 mA (a) and corresponding relative STD (b).....	41
Figure 25. The frequency response of the V_{in} at measured RMS currents from 10 nA to 5 mA (a) and corresponding relative STD (b).....	42
Figure 26. The frequency response of the V_{in} at measured RMS currents from 10 nA to 5 mA (a) and corresponding relative STD (b).....	42
Figure 27. Difference between the calculated and measured currents for various R_s values in the case of measured current 100 nA (a) and 10 nA (b), and R_{load} 100 Ω ..	43
Figure 28. Difference between the calculated and measured currents for various R_s values in the case of measured current 100 nA (a) and 10 nA (b), and R_{load} 10 k Ω ..	43
Figure 29. Difference between the calculated and measured currents for various R_s values in the case of measured current 100 nA (a) and 10 nA (b), and R_{load} 100 Ω ..	44
Figure 30. Difference between the calculated and measured currents for various R_s values in the case of measured current 100 nA (a) and 10 nA (b), and R_{load} 10 k Ω ..	44
Figure 31. Difference between the calculated and measured currents for various R_s values in the case of measured current 100 nA (a) and 10 nA (b), and R_{load} 100 Ω ..	44
Figure 32. Difference between the calculated and measured currents for various R_s values in the case of measured current 100 nA (a) and 10 nA (b), and R_{load} 10 k Ω ..	45
Figure 33. The difference of measured and calculated V_{in} for various measured currents at load resistance 100 Ω (a) and 10 Ω (b).....	47
Figure 34. The difference of measured and calculated V_{in} for various measured currents at load resistance 100 Ω (a) and 10 Ω (b).....	47
Figure 35. The difference of measured and calculated V_{in} for various measured currents at load resistance 100 Ω (a) and 10 Ω (b).....	47
Figure 36. The difference of measured and calculated V_{in} for various measured currents for ELP18 PC200 core with 10 turns (a) and for T50-26 core with 100 turns (b).....	48
Figure 37. The difference of measured and calculated V_{in} for various measured currents for T50-26 core with 30 turns (a) and 10 turns (b).....	48
Figure 38. The difference of measured and calculated V_{in} for the current range from 1 nA to 100 nA (a) and corresponding STD-s (b).....	48

List of tables

Table 1. Comparison of current sensing techniques [12] - [14]	24
Table 2. Difference between ferrite core and iron powder core [20]	29

1 Introduction

The subject of the thesis is the contactless measurement of small high-frequency currents, in particular, the sensitivity and accuracy of such measurements in synchronous measuring mode using a transformer. The expected frequency range is between 10 kHz and 5 MHz, and the current range is from 10 nA to 10 mA. Voltage source and serially connected precision resistors in the range from 100 Ω to 10 k Ω generate the measured current in a wire (single-turn primary winding of the transformer). The effect of the measuring circuit on the measured current should be examined [1].

Current sensing plays dominant role in the industrial world where current information can be used for controlling, monitoring and protection, thereby making current measurement very important. The classical approach of measuring current is by using a resistor and measuring the voltage drop across it. This method is good for small currents however when the current levels increase to large values, it becomes less efficient. This is because the power dissipation in the resistor increases with the current squared ($P = I^2R$). One solution for measuring large currents is by not directly measuring the current, but by measuring a property which is directly related to the current [2]. By measuring the voltage around a conductor, the current level can be calculated. In this thesis, low-level high-frequency current will be measured using a transformer in synchronous mode. The aim is to check its accuracy, sensitivity and resolution of the resulting current being measured. Comparative analysis of measurement results and a summary of the work. Recommendations for further research.

MFLI lock-in amplifier is configured with LabView will be used for this measurement. This is due to its capacity to extract signal amplitudes and phases in an extremely noisy environment [3].

1.1 Problem statement

There have been several methods for sensing current such as Shunt resistor, Rogowski current sensing, Hall effect, Fluxgate current sensing, Current transformer and others.

They all have their advantages and disadvantages which will be discussed in the following chapter. In this thesis, a transformer with a lock-in MFLI Amplifier will be used for current measurement. This is because in this thesis, measuring AC current is the interest. A lock-in amplifier is used in order to measure the amplitude and phase of the oscillating signal. A lock-in amplifier is also used to measure small signals that are buried in noise [3]. This is where the lock-in amplifier makes a difference as it combines techniques from the time and frequency domain analysis [3].

The aim of this current measurement with a transformer and MFLI lock-in amplifier is to measure current and to analyse what the result will be by taking note of its sensitivity, accuracy, and resolution. There will be a comparative analysis of measurement results, a summary of the work and recommendations for further research [1].

1.2 Frequency, amplitude and RMS (*Root Mean Square*) value

Frequency also known as alternating quantity is the total number of cycles made by a wave (sinusoidal) in one second. It is measure in cycle per second (c/s) or hertz (Hz) and the symbol is (f).

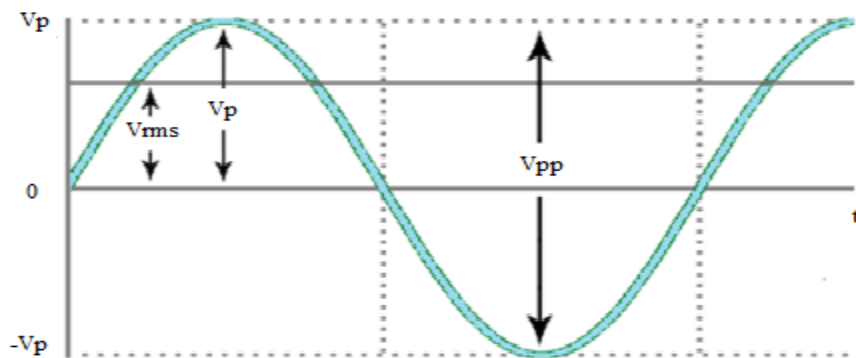


Figure 1. Voltage versus Time

1.3 Electromagnetic induction

Considering the title of this thesis, transformers makes use of electromagnetic induction to change the voltage of an electric current. For this reason, it is important to understand electromagnetic induction.

Electric field is defined as the force around the electrical charge particle. Force lines is found around the area of this field. The unit of electric field is in Volt/meter or Newton/coulomb and the symbol is E. It is perpendicular to the magnetic field. It is a vector quantity because it has magnitude and direction. On the other hand, when charges are moved, they create a magnetic field at a region called pole where there is an existence of force of attraction and repulsion. The unit of magnetic field is in Tesla and the symbol is B. Magnetic field is vertical to the electric field. It is also a vector quantity because it has magnitude as well as direction[4].

The combination of electric and magnetic field gives us electromagnetic field. According to encyclopedia Britannica, electromagnetic field is a property of space caused by the motion of an electric charge. A stationary charge will produce only an electric field in the surrounding space. If the charge is moving, a magnetic field is produced. An electric field can also be produced by a changing magnetic field. The mutual interaction of electric and magnetic fields produces an electromagnetic field [5]. Electromagnetic Induction is thus the ability of a magnetic field to generate current inside a conductor. This has been the foundation on which a transformer is designed.

1.4 Synchronous Measurement

Synchronous detectors can extract small signals, buried in the noise floor. In many systems, the noise increases as the frequency approaches zero. Moving the measurement away from the low-frequency noise increases the signal-to-noise ratio, allowing weaker signals to be detected. A narrow band-pass filter could remove all but the frequency of interest, allowing the original signal to be recovered. Alternatively, a synchronous demodulator can move the modulated signal back to DC while rejecting signals that are not synchronized to the reference. A device that uses this technique is called a lock-in amplifier [6].

One of the advantages of synchronous measurement is to reduce errors in measurement. Synchronized channels increase time resolution, making it possible to study time-dependent signals and their correlation. This makes the signal source stability less critical and further improves the signal to noise ratio [7].

The main advantage of synchronous measurement in our application is the possibility to use a narrowband filter, which allows to effectively suppress noise and interference on other frequencies, which allows to significantly improve the signal-to-noise ratio of the measured signal.

2 Current Sensing Techniques

In this chapter, various current sensing techniques and the features compared with the other measurement methods are provided. The current sensing techniques discussed in this chapter are shunt resistor, current transformer, Rogowski coil, fluxgate sensing and Hall Effect. They have their advantages and disadvantages in terms of sensitivity, accuracy, resolution size, bandwidth, precision, cost and the type of current they sense. These current sensing techniques gained their foundation from Ohm's law of resistance, Faraday's law of induction and magnetic field sensors [8].

2.1 Current sensing based on Ohm's Law of Resistance

Ohm's law of resistance is a derivative of Lorentz law which states that

$$J = \sigma (E + v * B) \quad (1)$$

where J is the current density, B the flux density, E is the electric field, v is the charge velocity and σ is the conductivity of the material. When the velocity of the moving charges tends to zero, Lorentz equation becomes

$$J = \sigma E \quad (2)$$

which is Ohm's law of resistance [8]. The current sensing technique that using Ohm's law of resistance is the shunt resistor. This method of sensing current is cheap compared to other current sensing technique.

2.1.1 Shunt Resistor

Shunt resistor is the classical way of measuring current because of its straightforwardness. The voltage drop across the shunt resistor increases as the current flowing through and decreases as the current decreases. This direct proportionality is measure of the current flowing through it. Shut resistor can be used to sense both alternating current (AC) and direct current (DC) [8].

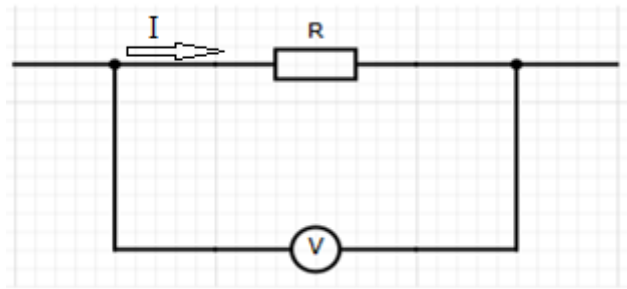


Figure 2. Shunt Resistor current sensing

where R is the resistance of the resistor in Ohms, V is the voltmeter and I is the current to be measured [9].

Advantages of shunt resistor:

- Very cost-effective solution
- Can work in AC and DC
- Additional equipment not required except for digital reading

Disadvantages of shunt resistor:

- Not suitable for higher current operation due to heat dissipation
- Shunt measurement provides an unnecessary decrease in system efficiency due to the energy wastage across the resistor
- In some cases, like impedance measurement, properties of the contact electrodes have a significant effect on the measurement result

2.2 Current sensing based on Faraday's Law of Induction

Current sensors founded on Faraday's law of induction provides electrical isolation which is the capacity to combine one circuit to the other directly without wires. This capacity allows the measurement of current on a high floating voltage [8].

2.2.1 Rogowski coil current sensors

In Rogowski coil current sensors, there is an air-core which is placed around the conductor which carry current. The magnetic field produced by the AC current induces a voltage in the coil. This voltage is proportional to the rate of change of current in the loop. The induced

voltage is passed through an integrator to produce an output voltage that is relative to the measured current. [10].

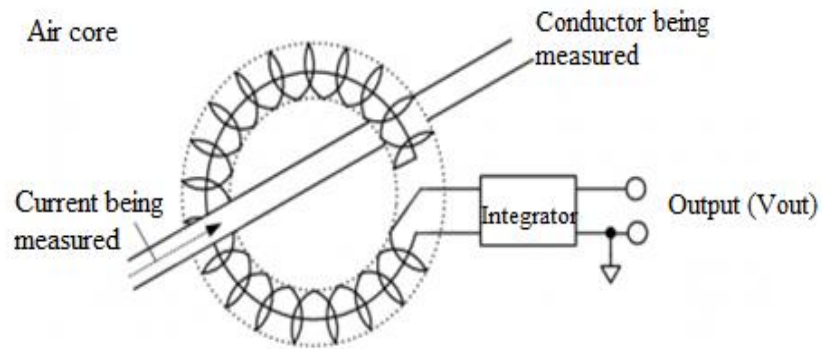


Figure 3. Rogowski coil current sensing

Advantages of Rogowski coil:

- Rogowski coil can measure large currents
- Rogowski coil current sensors have low impedance
- There is no hysteresis due to magnetic loss

Disadvantages of Rogowski coil:

- It can only measure AC current.
- Not suitable for precision measurement due to its susceptibility to external noise
- It cannot measure small current of 10 mA due to its coreless design

2.2.2 Current sensing using a Current Transformer

Current Transformer (CT) and Rogowski coil have an affinity as they operate on the principle of Faraday's law of Induction [8]. In CT the primary current that is being measured is converted to secondary current which is directly related to the turn's ratio [11].

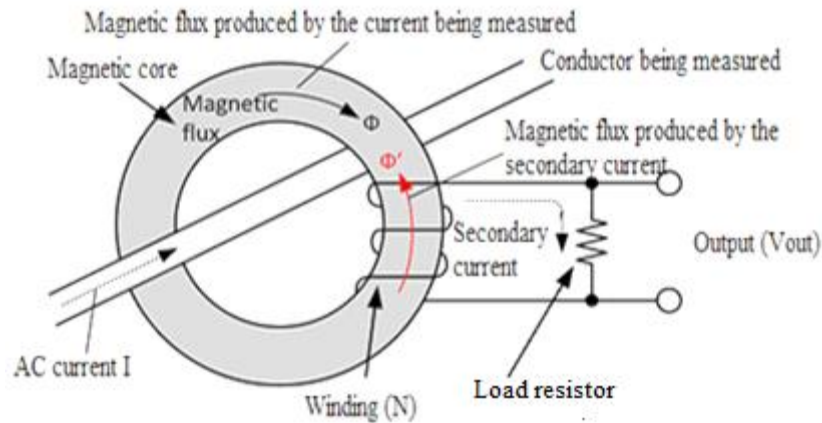


Figure 4. Current Transformer current sensing

Advantages of CT sensing [10],[11]:

- CT current sensors are inexpensive
- It can handle large current
- It has a low power consumption
- It is small in size
- CT current sensors are inexpensive

Disadvantages of CT sensing:

- The CT method can only measure AC current
- It has hysteresis due to its magnetization

2.3 Current sensing by means of Magnetic Field Sensors

Current sensors in the previous section that exploit Faraday's law of induction current sensors was discussed. These current sensors cannot sense current with static magnetic field. Magnetic field sensor which has the potential to sense current with static field as well as current with dynamic field is introduced. This dualism makes magnetic field current sensing attractive [8].

2.3.1 Hall Effect

In Hall Effect current sensing the magnetic field produced around the current being measured is converted to voltage. When current flow through a conductor, it produces mag-

netic flux inside the magnetic core. When this magnetic flux passes through the Hall element, it creates a voltage that is directly related to the magnetic flux. This voltage requires amplification to generate output signal because it is small. This output signal increases as the current in the conductor increases and decreases as the current in the conductor decreases [8].

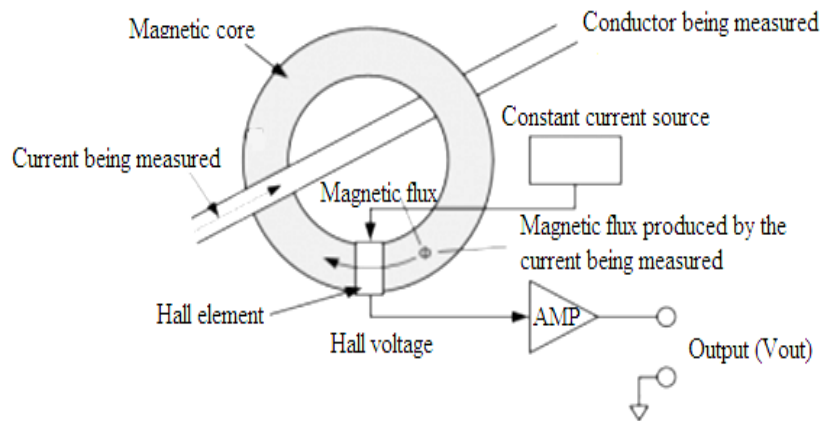


Figure 5. Hall Effect current sensing

Advantages of Hall effect:

- Hall element measures DC and AC current
- Hall current sensors are not expensive
- It is good for higher current measurement
- It has low power consumption

Disadvantages of Hall effect:

- It does not have a good precision due to hysteresis
- It sensitive to external magnetic field
- The voltage offset is large

2.3.2 Fluxgate Sensing

A saturable Inductor is the main component for the Fluxgate sensing technique. Due to this, Fluxgate sensor is called as Saturable Inductor Current Sensor. The inductor core which is used for the fluxgate sensor works in the saturation region. The saturation level of this inductor is highly sensitive, and any internal or external flux density changes the

saturation level of the inductor. The permeability of the core is directly proportional to the saturation level; hence the inductance also changes. This change in inductor value is analysed by the flux gate sensor to sense the current. If the current is high, the inductance become lower, if the current is low, the inductance become high [9].

The Hall Effect sensor works similarly to the fluxgate sensor, but there is one difference between them. The difference is probably that the saturation is avoided in the case of using Hall sensors.

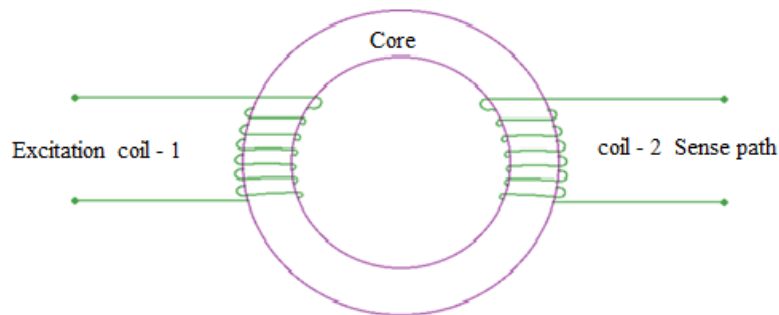


Figure 6. Fluxgate current sensing

In the diagram above, the basic construction of a flux gate sensor is shown. There are two coils primary and secondary wrapped around a saturable inductor core. The changes in the current flow can alter the core permeability resulting in the change of inductance across the other coil.

Advantages of Fluxgate:

- Has great accuracy
- Low offset and drifts with a high stability
- Delivers excellent linearity and maintains high precision down to low-level currents.

Disadvantages of Fluxgate

- High secondary power consumption
- A risk factor increases for voltage or current noise in the primary conductor.
- Only suitable for DC or low-frequency AC.

Fluxgate sensors are used in Solar Inverters to sense the current. Other than this, closed-loop AC and DC current measurement can be easily done by using Flux Gate sensors.

Flux Gate current sensing method can also be used in Leakage current measurement, overcurrent detection etc.

2.4 Comparison of the Current Sensors

Hall Effect current sensors have a sensitivity of about 1 mV/mT and fluxgate sensors have a sensitivity of hundreds of mV/mT. Hall sensors are not sensitive enough to be used in applications measuring low currents. Hall sensors also have higher offset voltages which only decreases the measuring capability of low currents. Fluxgate sensors can be used in low current measurements. Fluxgate are sensitive enough to measure currents of milliamperes. Rogowski coil has a low sensitivity than the current transformer [12] - [14].

Table 1. Comparison of current sensing techniques [12] - [14]

Current Sensing Techniques	Current Transformer	Rogowski coil	Hall Effect	Fluxgate	Shunt
Current Type	AC	AC	AC and DC	AC and DC	AC and DC
Current Range	High	Medium	Medium	High	Low
Accuracy	Medium	Low	Medium	High	High
Temperature Drift	High	Medium	Medium	Low	Low
High Current Measurement	Good	Good	Good	Very Good	Poor
Power Consumption	Low	Low	Low	Middle	High
Size	Small	Middle	Small	Middle	Very Small
Linearity	Fair	Good	Poor	Very Good	Good

3 Transformer

3.1 Transformers

An electric device consisting essentially of two or more windings, wound on a common core, which by electromagnetic induction transfers electric energy from one set of windings (primary) to another set of windings (secondary). While the voltage and current usually change (from primary to secondary), the frequency of the energy remains unchanged. Transformers only work on alternating current (not direct current). The voltage change is determined by the ratio of turns of wire around the core, between the primary and secondary windings [15].

Transformers increasing or decreasing the voltage and current supplied from the primary side without altering its frequency, or the amount of power being transferred from the primary winding down to the secondary winding [16].

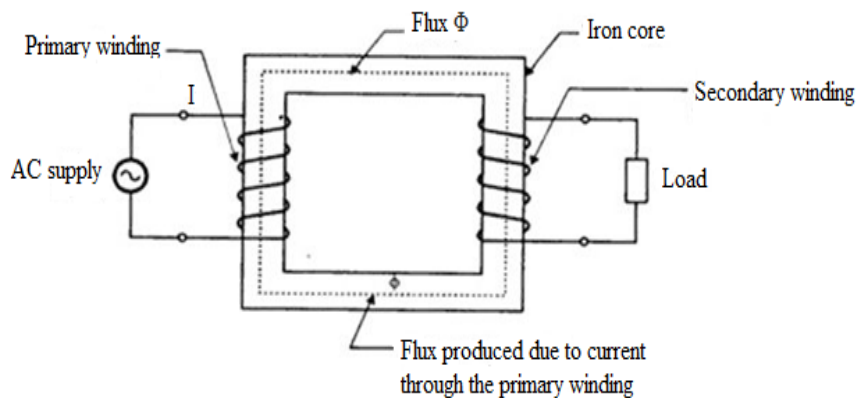


Figure 7. Single Phase Transformer Schematic [17]

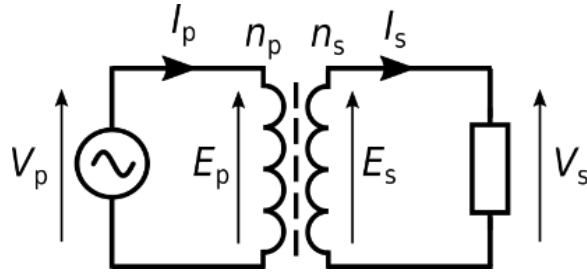


Figure 8. Simplified equivalent Circuit of a Transformer [1]

Transformers cannot be ideal. The ideal transformer is a simplified mode that does not consider the differences of real transformer. Ideal transformer does not consider core losses, copper losses due to resistance of the windings, magnetic flux leakage, stray capacitance. The core materials of real transformers have number of properties such as hysteresis, saturation effects and many parameters which depends on the operating frequency and temperature. The properties of winding wires depend on frequency (skin effect), temperature and so on [18].

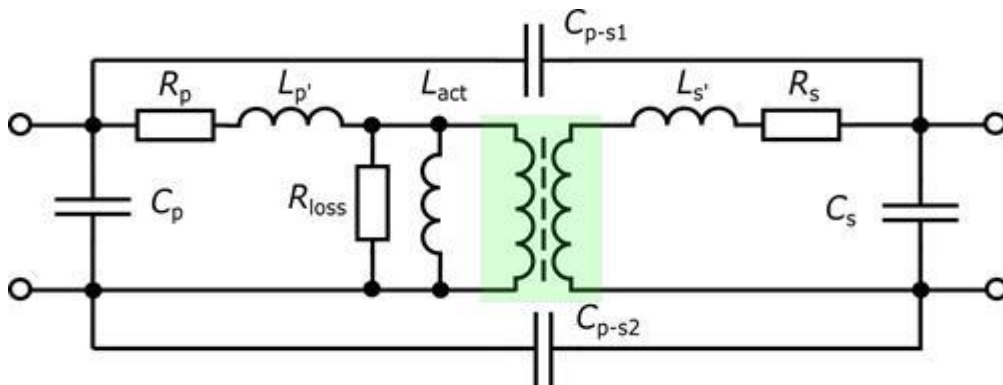


Figure 9. Simplified equivalent circuit of a real transformer [1]

The green portion of the circuit above denotes ideal transformer. Where, $L_{p'}$ and $L_{s'}$ denote leakage inductances of the primary and secondary side, L_{act} is inductance creating magnetization current, C_p and C_s are the primary and secondary capacitances, R_p and R_s are the primary and secondary resistances, C_{p-s1} and C_{p-s2} are capacitance from the primary side to the secondary and R_{loss} is resistance that takes care of non-zero iron losses.

3.2 Working Principles of a Transformer

Through electromagnetic induction, a transformer transfers electrical energy from one side of the circuit to the other side of the circuit. A varying current in one coil of the transformer produces a varying magnetic field, which in turn induces a varying electromotive force (EMF) or “voltage” in a second coil. Power can be transferred

between the two coils through the magnetic field, without a galvanic connection between the two circuits. Faraday's law of induction described this effect [19].

3.3 EMF Equation of Transformer:

The primary winding draws a current when it is connected to an alternating voltage source this sinusoidal current produces a sinusoidal flux Φ that can be expressed as [19]:

$$\Phi = \Phi_m \sin(\omega t) \quad (3)$$

where Φ_m is the maximum flux, ω is the angular frequency and t is time.

Instantaneous electromotive force (EMF) induced in the primary winding is:

$$e_1 = -N_1 \frac{d\Phi}{dt} \quad (4)$$

where $\frac{d\Phi}{dt}$ is change in flux with respect to time and e_1 is induced EMF in the primary side of the transformer.

Likewise, instantaneous emf induced in the secondary winding is:

$$e_2 = -N_2 \frac{d\Phi}{dt} \quad (5)$$

3.4 Transformer Turns ratio:

Turns ratio is an important parameter for drawing an equivalent circuit of a transformer. The turn ratio is used to identify the step-up and step-down transformers [19].

$$\frac{e_1}{e_2} = \frac{N_1}{N_2} = a \quad (6)$$

Where, a is the turns ratio of a transformer, N_1 is the number of the primary turns and N_2 is the number of the secondary turns.

If N_2 is greater than N_1 , the transformer is called a step-up transformer, whereas for N_1 is greater than N_2 , the transformer is called a step-down transformer. The losses are zero in

an ideal transformer. In this case, the input power of the transformer is equal to output power and this yield,

$$V_1 I_1 = V_2 I_2 = a \quad (7)$$

where V_1 and V_2 are primary and secondary voltages respectively.

The ratio of primary current to the secondary current is:

$$\frac{I_1}{I_2} = 1/a \quad (8)$$

The magneto motive force produced by the primary current will be equal to the magneto motive force produced by the secondary current and it can be expressed as:

$$N_1 I_1 = N_2 I_2 = a \quad (9)$$

3.5 Components of a Transformer

3.5.1 Transformer Core used

The cores use in this thesis are Amidon's iron powder toroidal T50-26 and the other is EPCOS/TDKELP 18x10 ferrite core with PC200 type ferrite.

Cores with 10, 30, and 100 secondary windings are used for measuring current in this thesis.



Figure 10. Cores with secondary windings

- Amidon's iron powder toroid T50-26, $D = 12.7$ mm, $d = 7.62$ mm, $h = 5$ mm, $\mu_e = 75$, $AL = 33$ nH, 10 turns, wire diameter 0.5 mm, $R_s = 39.6$ m Ω , $L = 4.064$ μ H (@ 29.15 kHz),

- The same as 1 with 30 turns, wire diameter 0.5 mm, $R_s = 149.7 \text{ m}\Omega$, $L = 32.86 \text{ }\mu\text{H}$ (at 16.3 kHz),
- The same as 1 with 100 turns, wire diameter 0.5 mm, $R_s = 5.38 \text{ }\Omega$, $L = 341.3 \text{ }\mu\text{H}$ (at 52.14 kHz),
- EPCOS/TDK ELP 18x4x10 ferrite core, PC200 material with 118x2x10 cap (also PC200) $\mu\epsilon = 640$, $AL = 1300 \text{ nH}$, 10 turns, wire diameter 0.25 mm, $R_s = 272.8 \text{ m}\Omega$, $L = 142.6 \text{ }\mu\text{H}$ (at 298.4 kHz).

Impedance data is collected with Wayne Kerr 6500B Precision Impedance Analyzer. Data collection interval 20 seconds, series measurement mode with 10 mA excitation current, with (100) frequencies in the range from 1 kHz to 100 MHz.

Table 2. Difference between ferrite core and iron powder core [20]

Ferrite core	Iron powder core
Ferrite has a higher resistivity	Iron powder has a lower resistivity
It has a higher dielectric property	It has a lower dielectric property
It has a higher permeability	It has a lower permeability
Ferrite has a low saturation magnetization which limits its application at low frequency	Iron powder has a high magnetization
Ferrite core for common mode	Iron powder for differential mode
Ferrite for high frequency but not DC	For low frequency can be DC

3.5.2 Inductor

An inductor is a device that stores energy in form of a magnetic field. It has a symbol L and it is measured in Henry. The inductance of an inductor is the property of an electric conductor that causes an EMF to be generated by change in the current flowing through it. This EMF is often called counter EMF because it opposes the variation of current. When current passes through a coil it generates a magnetic field with varying magnetic flux. This is known as self-inductance. When a nearby coil is placed closer to this coil, the varying magnetic flux links with the nearby coil creating a mutual inductance between the coils [21]. A transformer makes use of mutual inductance for its operation.

4 Measurement Setup and Results

4.1 Introduction of MFLI Lock-in Amplifier

A Lock-in amplifier is a type of amplifier with the ability of extracting a signal with a known carrier wave from a very noisy environment. It is used to measure the amplitude and phase of an oscillating signal. A lock-in measurement extracts signals in a defined frequency band around the reference frequency, efficiently rejecting all other frequency components. Over decades of development, researchers have found many ways to use lock-in amplifiers. Most prominently they are used as precision AC voltage and AC phase meters, noise measurement units, impedance spectroscopes, network analysers, spectrum analysers and phase detectors in phase-locked loops. The lock-in detection technique is described both in the time and in the frequency domain. As essential as spectrum analysers and oscilloscopes, they are work horses in all kinds of laboratory setups, from physics to engineering and life sciences [3].

4.1.1 Lock-in Amplifier working principle

Lock-in amplifiers use the knowledge about a signal's time dependence to extract it from a noisy background. A lock-in amplifier performs a multiplication of its input with a reference signal, also sometimes called down-mixing or heterodyne/homodyne detection, and then applies an adjustable low-pass filter to the result. This method is termed demodulation or phase sensitive detection and isolates the signal at the frequency of interest from all other frequency components. The reference signal is either generated by the lock-in amplifier itself or provided to the lock-in amplifier and the experiment by an external source. The reference signal is usually a sine wave but could have other forms, too. Demodulation with a pure sine wave enables selective measurement at the fundamental frequency or any of its harmonics. Some instruments use a square wave which also captures all odd harmonics of the signal and, therefore, potentially introducing systematic measurement errors [3].

4.1.2 Summary of MFLI Lock-in Amplifier

The MFLI Lock-in Amplifier uses the latest hardware and software technologies to bring the benefits of high-performance digital signal processing to lock-in amplifiers at low and medium frequencies. The MFLI covers the frequency ranges DC to 5MHz [22].

4.1.3 Description of MFLI Lock-in Amplifier

The differential voltage and current inputs of the MFLI are optimized for low noise operation down to very low frequencies, and the high oversampling ensures high SNR. Both current and voltage signals can be measured simultaneously, facilitating 4-terminal measurements for instance. At the output the MFLI can generate a low distortion sinusoidal signal of up to 10 V capable to drive your device under test. Voltage and current measurements are supported by MFLI [23].

4.2 Measurement setup

The measurements are done with an automatic measuring system which is configured using LabView for measurement using current transformer. The setup consists of:

- a Zurich Instrument MFLI lock-in Amplifier with 5MHz and 60MSa/s,
- a current Transformer with a core having a single conductor passing through the core as the primary turn and a secondary winding with different number of turns according to the number of measurements taken, a precision resistor, a load resistor, connectors and metal casing for shielding,
- a PC (*personal computer*) system with software for controlling of MFLI parameters and recording measurement results,

The measured current is obtained from a voltage source, the voltage of which is set so that, it together with the resistors R_{out} , R_{in_i} and R_{ext} present in the circuit, generates a predetermined current (see Figure 12). This current is also measured by the current input of the MFLI, shown in the figure as an ammeter A.

The transformer is connected to the MFLI with one end of the precision resistor with the conductor carrying current in the primary side is connected to the current input signal and the other end together with the precision resistor is connected to the signal output voltage.

The terminals of the secondary turns are connected to -V Diff (differential voltage) and +V together with the load resistor. The figure below shows the setup:

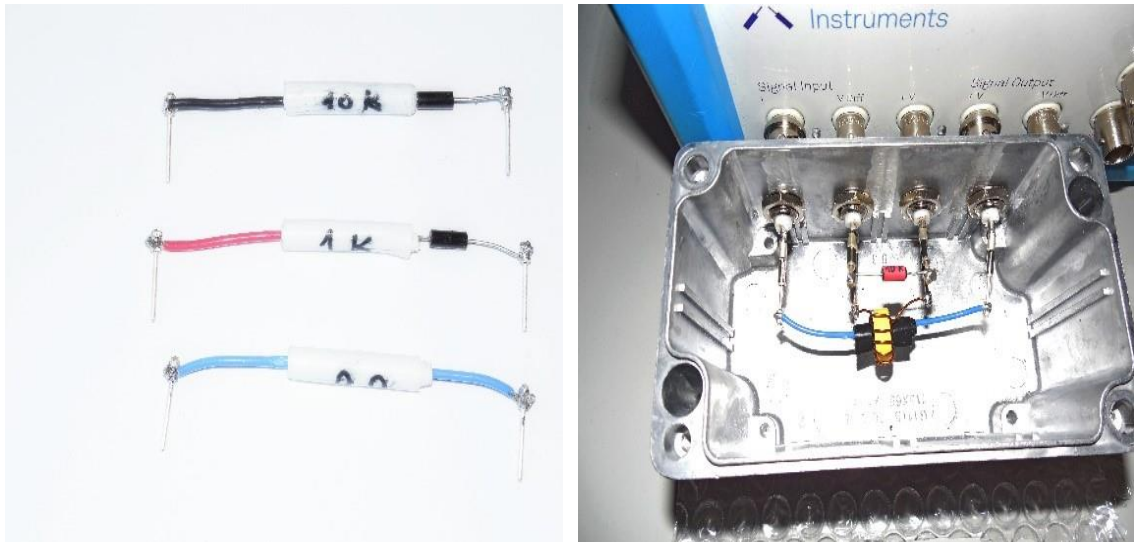


Figure 11.(a) series resistor, and (b) measurement setup

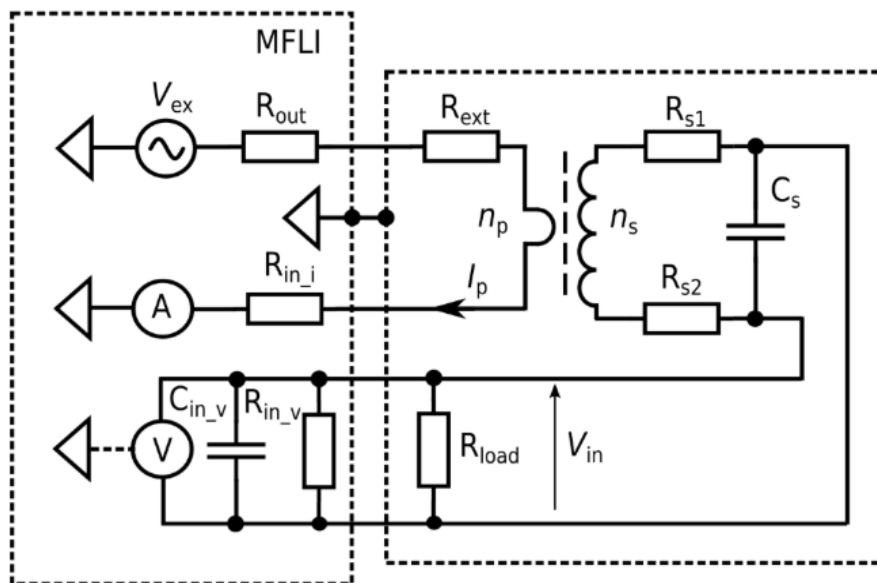


Figure 12. Simplified measurement circuit

4.3 Procedure

The primary winding is either a straight wire or a single loop to which a series resistor is connected in series. The series resistor determines the impedance of the circuit as well as the current to be measured since a voltage source is connected in series with this resistor. The series resistor can have three values 100 Ω , 1 k Ω and 10 k Ω . 100 Ω is formed by the input and output impedance of the measuring instrument (Zurich Instrument MFLI).

Primary turns with series resistors (a) and transformer connections to MFLI lock-in amplifier (b). The measuring circuit is located in a screening box (with the cover removed in the picture). The reason for using the box is to minimize noise from the environment.

The red component is the load resistor R_L connected in parallel with the secondary turns and the voltage measurement input. R_L is varied in the range from $10\ \Omega$ to $1\ \text{M}\ \Omega$. It should be noted that $1\ \text{M}\ \Omega$ and $100\ \Omega$ is formed by the selectable input impedance of the measuring instrument.

4.3.1 Impedance data of secondary turns

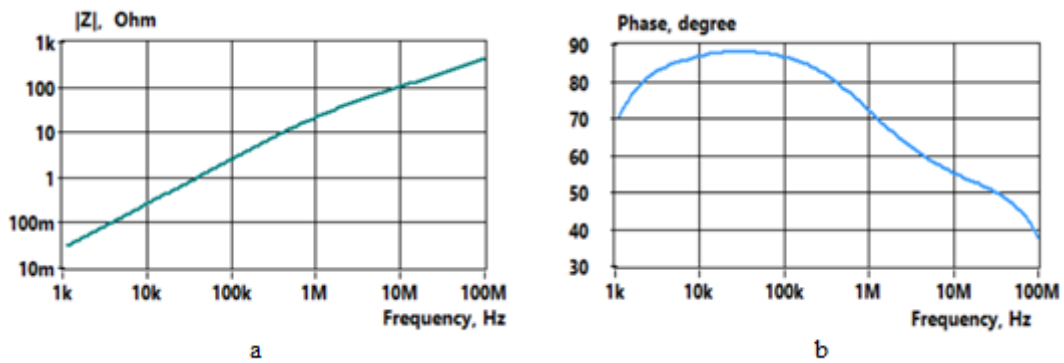


Figure 13. Impedance magnitude (a) and Phase (b) with 10 turns for T50-26 core

The shape of the impedance magnitude and phase indicates the significant core losses at frequencies above 100 kHz.

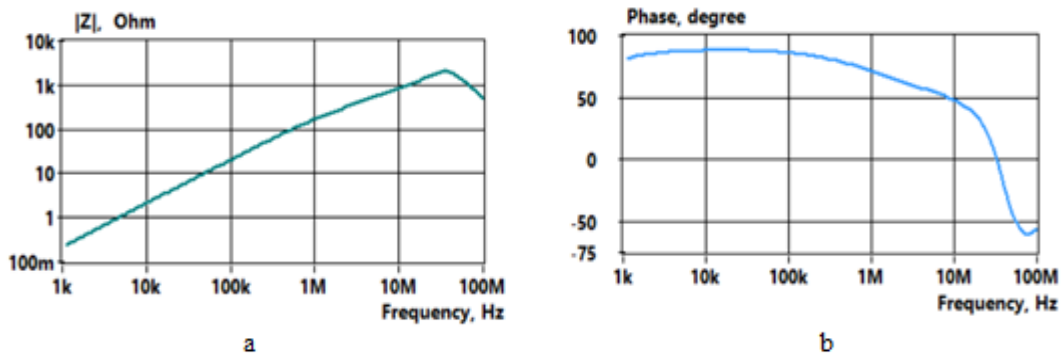


Figure 14. Impedance magnitude (a) and Phase (b) with 30 turns for T50-26 core

The core losses are also noticeable. Parallel resonance at 35.1 MHz.

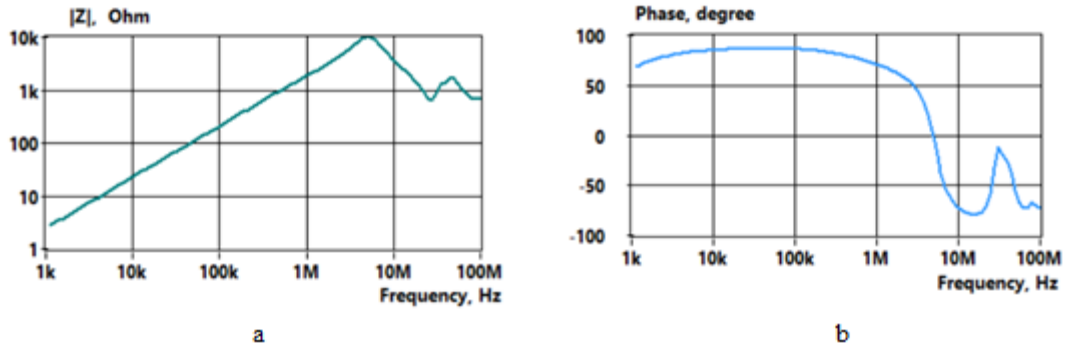


Figure 15. Impedance magnitude (a) and Phase (b) with 100 turns for T50-26 core

The core losses are also noticeable. Parallel resonance at 4.68 MHz, and series resonance at 27.8 MHz.

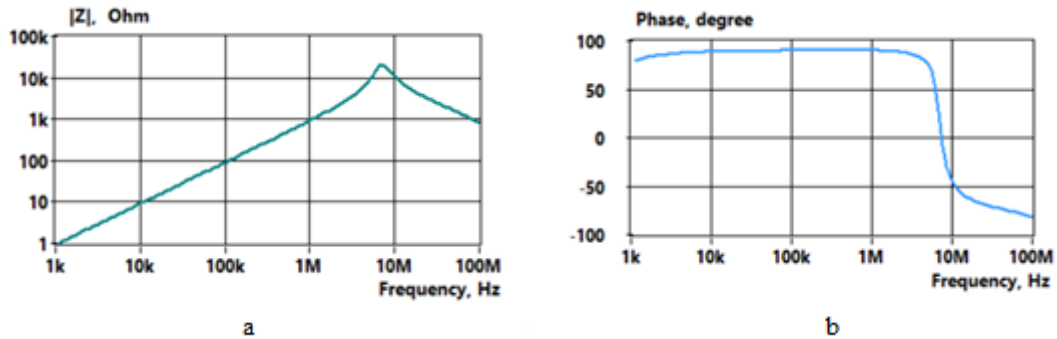


Figure 16. Impedance magnitude (a) and Phase (b) with 10 turns ELP 18 PC200 core

No significant core losses are also noticeable. Parallel resonance at 6.89 MHz.

4.4 Results and Analysis

4.4.1 Introduction to the current measurement with a transformer

A wire that carries an electric current creates the concentric magnetic field lines around it. The use of magnetic cores with relative permeability $\mu \gg 1$ allows the concentration of the magnetic flux inside the measurement coil.

In the case of the toroidal magnetic core, the magnetic field H produced by single wire along its axis can be obtained from Ampere's law:

$$\oint H dl = i_p - n_s i_s \tag{10}$$

where l is the mean path length around the core, i_p and i_s are the primary and secondary currents, and n_s is a number of secondary turns. If the cross-section of the core is small compared to the radius, the field in the core due to the currents is nearly uniform; it can then be integrated around a closed path inside the core and obtain:

$$H = (i_p - n_s i_s) / l \quad (11)$$

Using now the magnetic flux density $B = \mu H$ and effective cross-sectional area of the core, the flux in the core Φ and the voltage V at the coil with the load resistor R can be calculated:

$$\Phi = B A = \mu A (i_p - n_s i_s) / l \quad (12)$$

$$V = n_s d\Phi / dt = i_s R \quad (13)$$

Combining (12) and (13) the following differential equation can be obtained for the secondary current i_s :

$$i_s R = (n_s^2 \mu A / l) d / dt (i_p / n_s - i_s) \quad (14)$$

Where, $n_s^2 \mu A / l = L$ is the inductance of the coil and therefore,

$$di_s / dt + i_s R / L = (1 / n) di_p / dt \quad (15)$$

When the coil is terminated with a low impedance, the induced voltage becomes irrelevant, and the coil current and the load resistance instead determine the output voltage. The mid-band transfer resistance, or sensitivity, G , is equal to R/n_s , where R is the termination resistance (R_{load}). The above formulas are based on the description given in [24].

For higher sensitivity, an additional low noise amplifier should be used. In this case, ZI MFLI lock-in amplifier is used for that purpose. It is impractical to arbitrarily increase the sensitivity of a passive current monitor. To increase G , one would increase R , which increases the thermal noise or decrease n_s , which would increase the low cut-off frequency f_L , as described in section 4.4.2. The thermal noise voltage V_n is calculated as:

$$V_n = \sqrt{4kTbR} \quad (16)$$

where k is Boltzmann's constant, T the absolute temperature, R the resistance of the circuit element and b the frequency bandwidth.

4.4.2 The frequency response

PSpice modelling results with Micro-Cap 12 illustrate the frequency response of the voltage V_{in} and its phase curves when R_{load} is varied in the range from 10Ω to $10 \text{ k}\Omega$. Input current is $1 \mu\text{A}$, and the number of secondary winding $n_s = 10$.

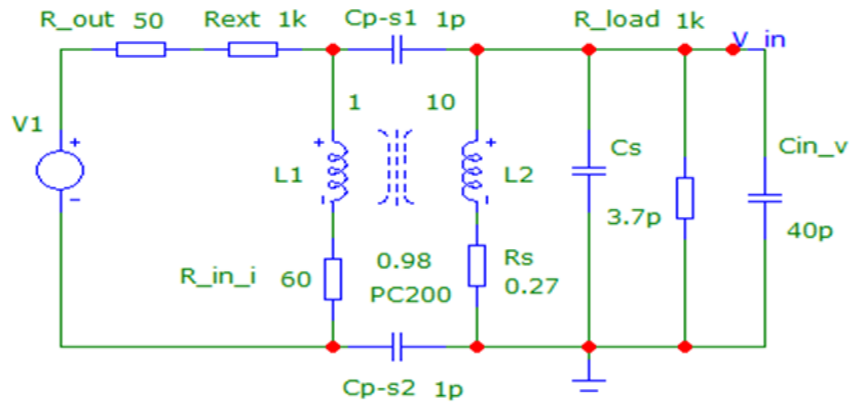


Figure 17. Equivalent circuit of the measurement setup

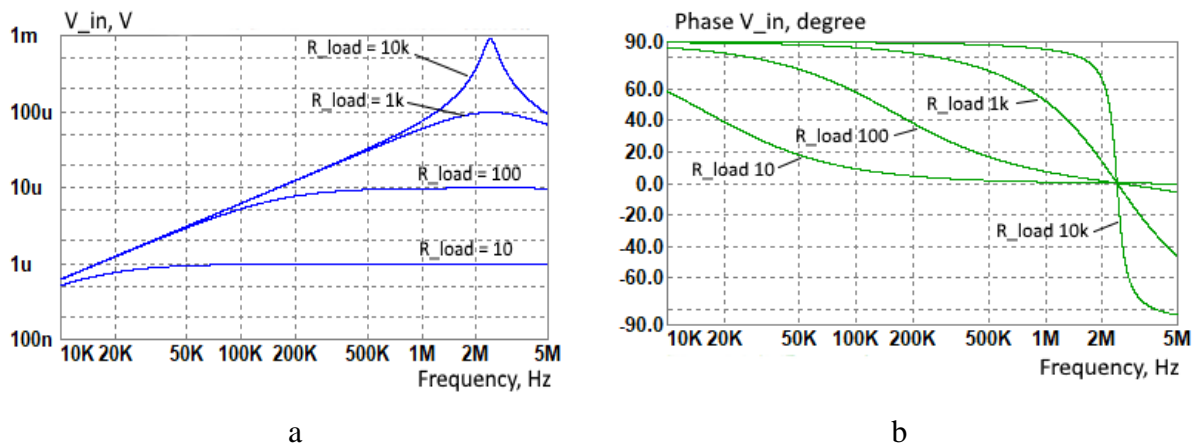


Figure 18. Modelled frequency response of the V_{in} (a) and corresponding phase response (b)

The results of experimental measurements under similar conditions:

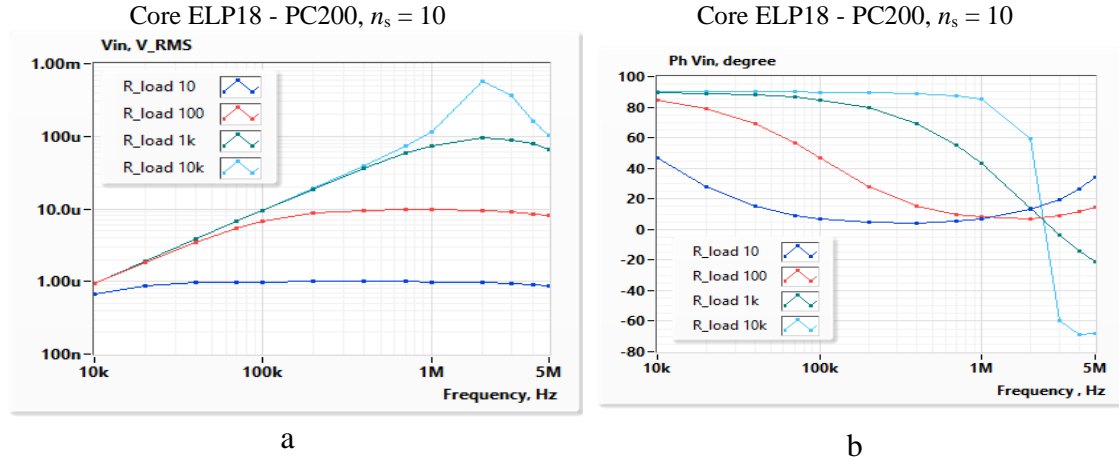


Figure 19. The measured frequency response of the V_{in} (a) and corresponding phase response (b)

In the case of high load resistance values, the voltage V_{in} (output voltage V at the terminals of the coil) increases almost linearly close to the resonance area. The resonant frequency f_r is determined by the inductance of the coil L and total capacitance C in parallel with it. In practical experiments, the total capacitance is formed as a sum of self-capacitance of the coil C_s and input capacitance of the amplifier (measurement instrument, ZI MFLI) C_{in_v} .

$$f_r = \frac{1}{2\pi\sqrt{LC}} \quad (17)$$

Near the resonance, the voltage is significantly affected by its properties, which are not well determined in advance. The Q factor of resonance depends on the loss of the core; the frequency of resonance depends on the parasitic capacitances. Since the core losses depend on the frequency (increase with frequency), it is not a normal resistance but a frequency-dependent resistance. It should be noted that in the equivalent circuit, the element describing the core losses is omitted. In the case of higher losses (as with T50-26 cores), the losses have a considerable impact (this can be monitor on the impedance plots measured with Wayne-Kerr analyzer). However, it is not easy to find or calculate parameters from this data for the equivalent circuit. So currently, it should be noted that there is an influence.

Above the resonance frequency, the influence of the capacitance causes the output signal to drop. Loading of the coil with a smaller resistance R exhibits a frequency characteristic with a plateau between the low corner frequency f_i

$$f_l = (R_s + R) / 2\pi L \quad (18)$$

and the high corner frequency f_h

$$f_h = 1 / 2\pi R_s C \quad (19)$$

The current sense transformer operates the same as any transformer, with the exception that the primary signal is current. The primary-to-secondary current relationship is given

$$\frac{i_s}{i_p} = \frac{n_p}{n_s} \quad (20)$$

It follows that in case of $n_p = 1$ $i_s = i_p n_s$, and in the frequency range f_l to f_h , the output voltage V (that is also the input voltage of following amplifier V_{in}) is defined by the load resistor R_L and number of turns n_s :

$$V_{in} = \frac{i_p R_L}{n_s} \quad (21)$$

Since the number of turns is constant for a particular transformer, V_{in} directly depends on primary current and load resistance. However, the current in the primary is transformed through the action of the magnetizing current that is supplied by the primary and is therefore subtracted from the current available to drive the secondary. This leads to several design criteria for the transformer. Low magnetizing current provides uniform secondary current, and this is achieved by providing a large inductance. Large inductance can be achieved by using a core with higher permeability and (or) more turns of the coil. Unfortunately, both methods have limitations at higher frequencies. The permeability of core materials decreases with frequency. A higher number of turns results in higher series resistance and capacitance, as well as increased dimensions. A lower number of turns at the same magnetic permeability limits the sensitivity in the lower frequency range.

It is possible to use the transformer also below the low corner frequency f_l expressed by (18). It should be noted that f_l can be shifted higher by using a high value of R_{load} . In this case, the voltage at terminals of the secondary coil can be calculated as

$$V_{in} = \frac{2\pi f L i_p}{n_s} \quad (22)$$

The results of experimental measurements with R_{load} 100 k Ω , core ELP18 18x4x10 PC200 ferrite, the number of turns $n_s = 10$, $R_s = 1$ k Ω is illustrated in Figure 20:

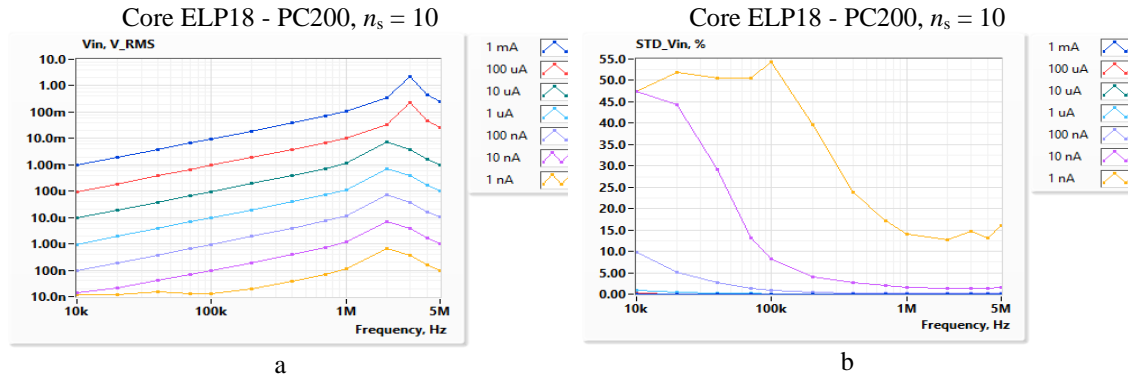


Figure 20. The frequency response of the V_{in} at measured RMS (*Root mean Square*) currents from 1 nA to 1 mA (a) and corresponding relative STD (*Standard Deviation*) (b) with R_{load} 100 k Ω

The inductance of the coil is 142.6 μ H. Due to the low level of the V_{in} at low currents and low frequencies, STD increases significantly. However, the results are quite acceptable for 10 nA above 5 MHz and even for 1 nA in the range from 1 to 5 MHz. In Figure 21 measurement results under the same conditions, except for R_{load} 100 Ω , are presented for the comparison.

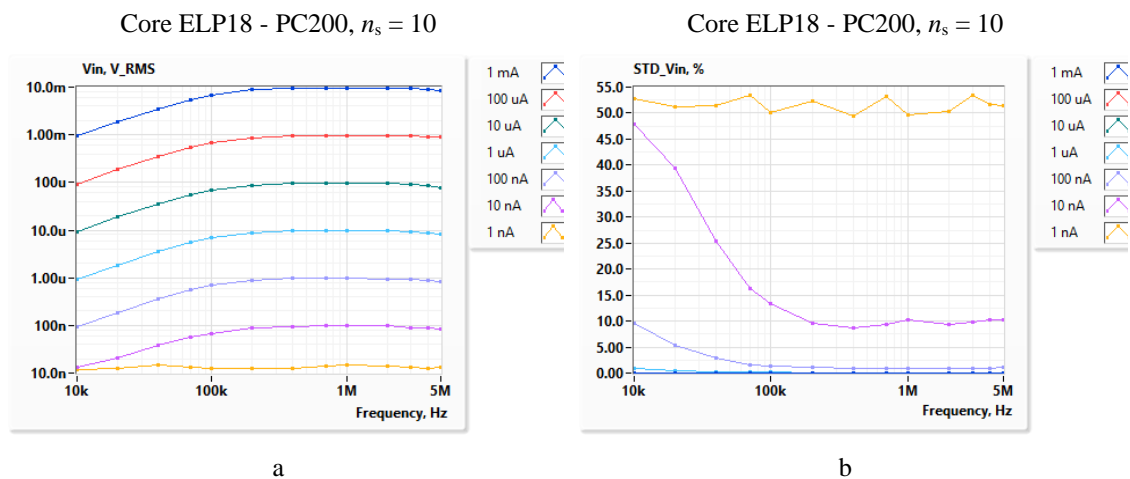


Figure 21. The frequency response of the V_{in} at measured RMS currents from 1 nA to 1 mA (a) and corresponding relative STD (b) with R_{load} 100 Ω

The current 1 nA is not measurable when employing R_{load} 100 Ω . For 10 nA, STD is significantly higher at frequencies above 100 kHz and is also higher for 100 nA above 100 kHz. It may be concluded that the use of high R_{load} measurement mode is beneficial for ≤ 100 nA at frequencies above 100 kHz. The influence of higher thermal noise level, according to (16), is effectively suppressed by filtering in the ZI MFLI lock-in amplifier. The drawback of using high R_{load} is that the measurement result is influenced by resonance. To minimize the related inaccuracy, all the parameters related to resonance (e.g., stray capacitances, core losses) should be well determined and kept constant during the measurement.

The compromise is to use an average R_{load} value of 1 k Ω . As can be seen in Figure 22, small currents are measurable in some higher frequency range, but the effects of resonance are significantly smaller.

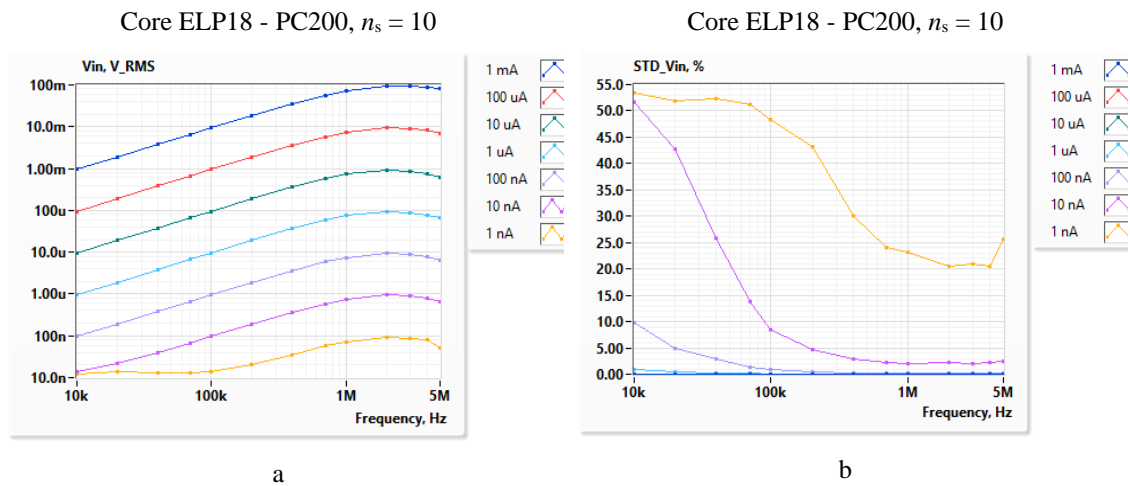


Figure 22. The frequency response of the V_{in} at measured RMS currents from 1 nA to 1 mA (a) and corresponding relative STD (b) with R_{load} 1k Ω

In addition to the relationships described above, there is another parameter for a particular task that distinguishes it from the many common current measurement tasks. It is typically assumed that the current source provides a “constant,” unalterable current that depends little on the characteristics of the measuring transformer. However, this is not the case of a current task, because the measured current is obtained from a voltage source whose internal resistance varies from 100 Ω to 10 k Ω . Therefore, the measurement circuit may significantly affect the measured current through the feedback. One of the tasks of the work is to study such effects.

4.4.3 Comparison of the frequency response of V_{in} and STD with different cores and number of turns

In Figure 23 to Figure 26, the frequency response of the V_{in} at measured RMS currents from 10 nA to 5 mA and corresponding relative standard deviation (STD) with different cores and the number of secondary turns is illustrated. R_{load} 1 k Ω and total series resistance $R_s = 1.11$ k Ω on the primary side of the transformer.

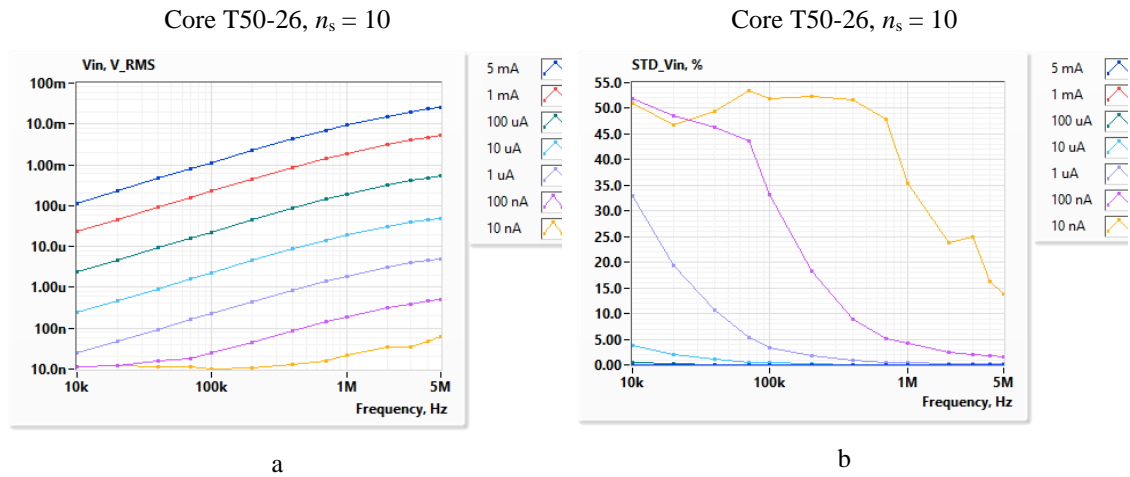


Figure 23. The frequency response of the V_{in} at measured RMS currents from 10 nA to 5 mA (a) and corresponding relative STD (b)

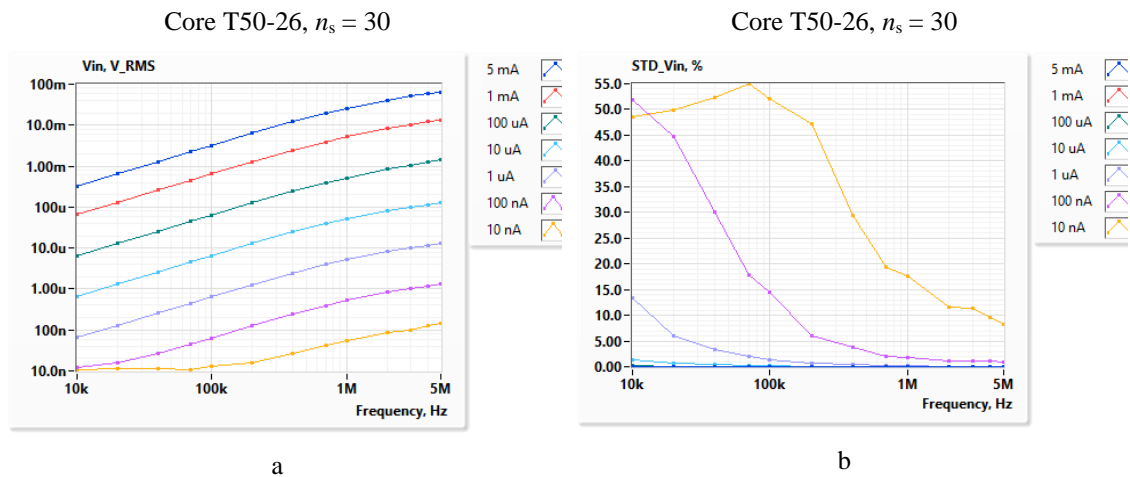


Figure 24. The frequency response of the V_{in} at measured RMS currents from 10 nA to 5 mA (a) and corresponding relative STD (b)

Based on the data in Figures 23 to 24, it can be concluded that the sensitivity of the current measurement increases in proportion to the number of secondary turns as expected. It can also be concluded that the large measurement errors make the results with 10 nA current practically useless in the case of 10 and 30 turns of the T50-26 secondary winding. For 100 nA, the measurement errors are significantly less at frequencies above 100 kHz. The

coils with 10 and 30 turn are better suited for higher currents and have the advantage over the 100-turn coil is the lack of resonance effects.

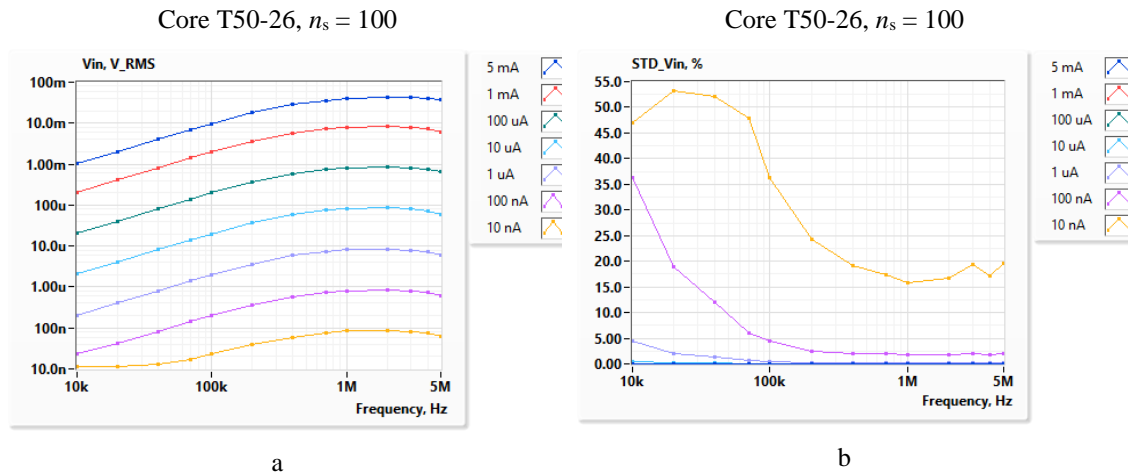


Figure 25. The frequency response of the V_{in} at measured RMS currents from 10 nA to 5 mA (a) and corresponding relative STD (b)

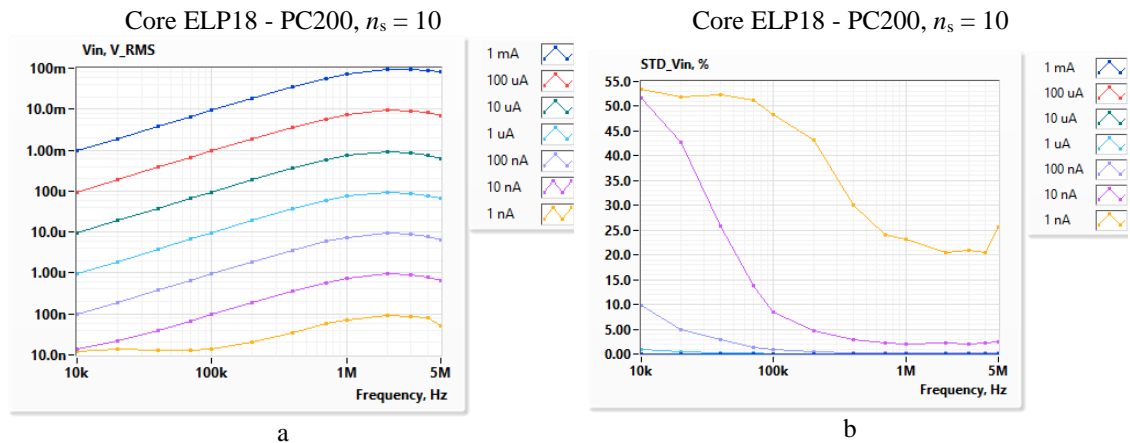


Figure 26. The frequency response of the V_{in} at measured RMS currents from 10 nA to 5 mA (a) and corresponding relative STD (b)

The advantages of using a low loss core with a higher permeability can be expressively seen from Figures 25 and 26. A transformer with ten times fewer turns provides almost twice the sensitivity.

4.4.4 The influence of the series resistance on the primary side of the transformer

As already discussed in the introductory section, the measured current is obtained from a voltage source whose internal resistance varies from 100 Ω to 10 k Ω . Therefore, the measurement circuit may significantly affect the measured current through the feedback. To evaluate the effect of the measurement scheme on the measured current I_{in} , the

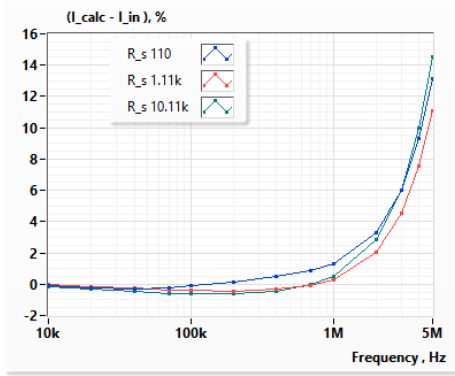
difference between the measured current and the calculated current I_{calc} . can be used. I_{in} is measured with ZI MFLI current input, and I_{calc} can be found as

$$I_{calc} = \frac{V_{ex}}{R_s} = \frac{V_{ex}}{R_{out} + R_{ext} + R_{in_i}} \quad (23)$$

where V_{ex} is the output voltage, R_{out} its output resistance (typically 50 Ω) R_{in_i} is the input resistance of the current measurement input (typically 50 Ω or 60 Ω) and R_{ext} the resistance of external precision resistor (1 k Ω , or 10 k Ω).

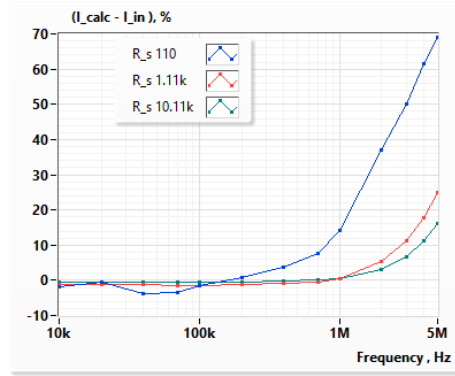
The percentage difference between the calculated and measured currents for various R_s values and R_{load} 100 Ω and 10 k Ω is shown in Figure 27 to Figure 32.

Core ELP18 - PC200, $n_s = 10$, R_{load} 100 Ω



a

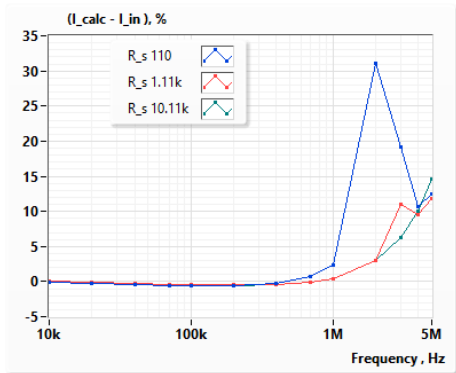
Core ELP18 - PC200, $n_s = 10$, R_{load} 100 Ω



b

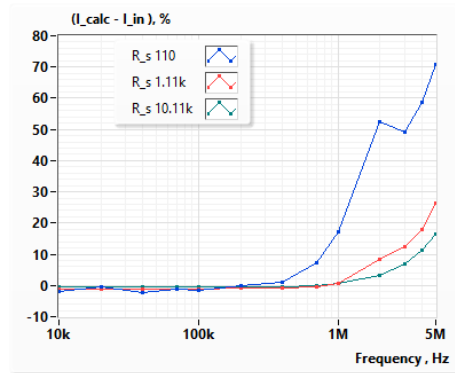
Figure 27. Difference between the calculated and measured currents for various R_s values in the case of measured current 100 nA (a) and 10 nA (b), and R_{load} 100 Ω

Core ELP18 - PC200, $n_s = 10$, R_{load} 10 k Ω



a

Core ELP18 - PC200, $n_s = 10$, R_{load} 10 k Ω



b

Figure 28. Difference between the calculated and measured currents for various R_s values in the case of measured current 100 nA (a) and 10 nA (b), and R_{load} 10 k Ω

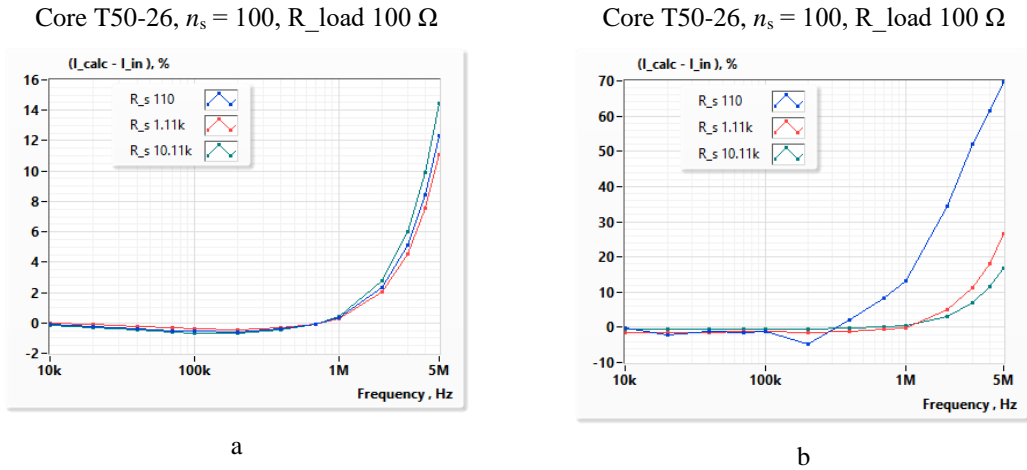


Figure 29. Difference between the calculated and measured currents for various R_s values in the case of measured current 100 nA (a) and 10 nA (b), and R_{load} 100 Ω .

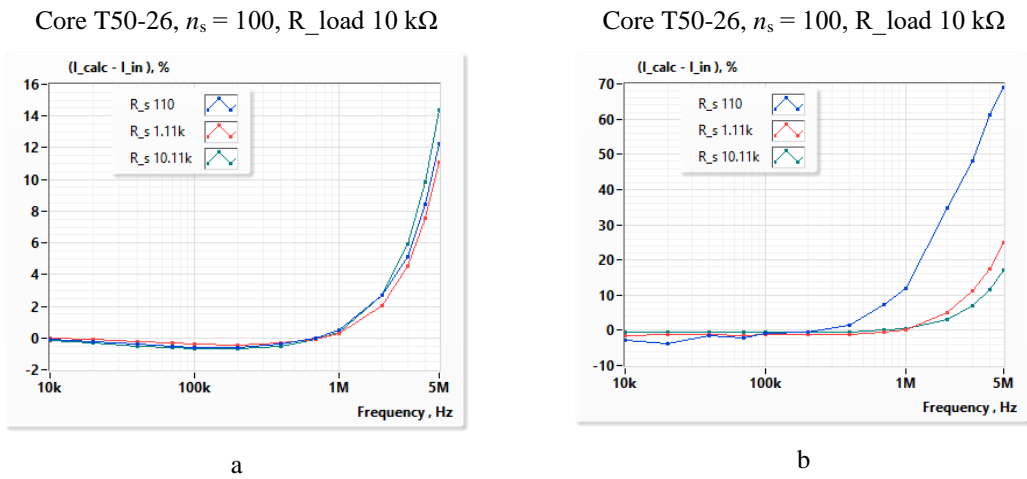


Figure 30. Difference between the calculated and measured currents for various R_s values in the case of measured current 100 nA (a) and 10 nA (b), and R_{load} 10 k Ω .

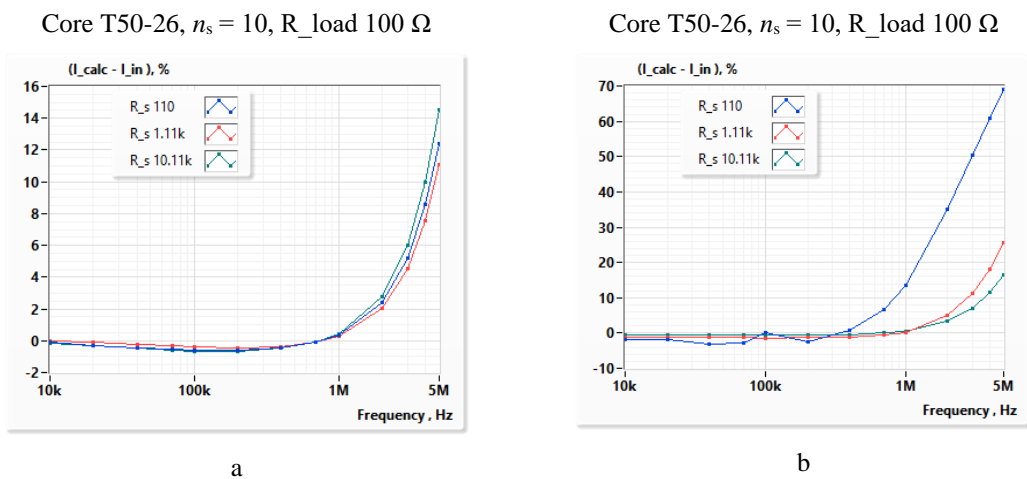


Figure 31. Difference between the calculated and measured currents for various R_s values in the case of measured current 100 nA (a) and 10 nA (b), and R_{load} 100 Ω

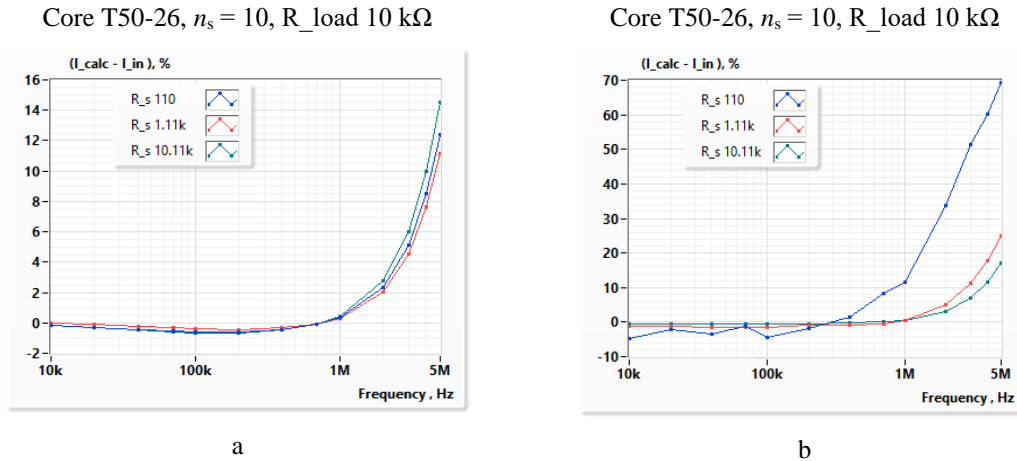


Figure 32. Difference between the calculated and measured currents for various R_s values in the case of measured current 100 nA (a) and 10 nA (b), and R_{load} 10 k Ω

A comparison of the measurement results shows that the effect of the load on the secondary side of the measuring transformer the input current depends on the series resistance R_s of the primary side. This effect increases with the frequency, where it causes a significant decrease in the measured current. It is also evident that the effect of R_s changes direction at the centre frequencies. One possible reason is an increase in core losses at higher frequencies.

The large jumps of the current difference in Figure 28 occur near the resonance, where the impedance of the secondary side changes abruptly. For T50-26 cores, this effect does not occur because higher core losses attenuate the Q factor of the secondary circuit.

Part of the current difference may also be related to errors caused by the instrument used, as according to the specification, the accuracy of the output voltage is guaranteed by 1% up to 500 kHz and the same accuracy of current measurement up to 100 kHz.

4.4.5 Measurement errors.

To estimate the systematic error of the currents measured in the experiments, a comparison of the measured input voltage V_{in} with their calculated values using formulas (21) and (22) is made.

Formula (21) can be used for uniform frequency response, between the cut-off frequencies f_l and f_h . Approximately this situation is achieved with low ohmic load resistances of 10 Ω and 100 Ω . Alternatively, formula (22) can be used in a uniformly increasing portion of the frequency response, before the resonant frequency. To achieve this situation, a high ohmic load of 10 k Ω can be used.

Since, in both cases, a precision resistor with a tolerance of $\pm 0.1\%$ is used for the load, the primary source of error in finding the calculated value of V_{in} is the tolerance of the winding inductance L , which is approximately $\pm 2\%$.

The measurements discussed in this work are associated with two types of measurement errors: systematic error which can be reduced by calibration and random error which can be reduced by averaging. To calculate systematic error, it would be necessary to know the actual value of the current. Unfortunately, it is not possible to know the exact current values. Instead, two more accurate values are known that can be used as references:

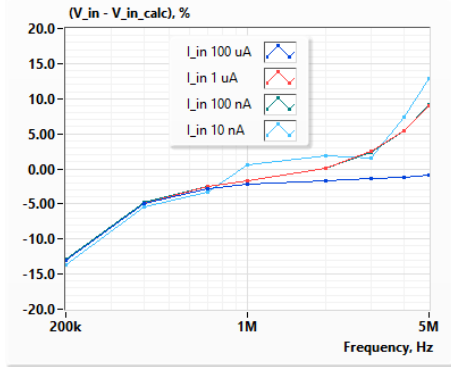
- Calculated current value I_{calc} based on the ratio of known excitation voltage to the total resistance in the primary side of the transformer. The accuracy of this reference current is determined by two components: 0.1% accuracy of used resistors and the accuracy of V_{ex} generated by MFLI. Unfortunately, data on the accuracy of the MFLI output voltage is limited. It is only known that it is below 1% at frequencies up to 100 kHz. Because the errors are independent, total systematic error can be calculated as the square root of the sum of the squares of both values, which still gives nearly 1% at frequencies up to 100 kHz. At higher frequencies, this number is higher, but probably not more than 5%.
- Current measured with MFLI current input. The systematic error of this measurement is also below 1% at frequencies up to 500 kHz.

It may be concluded that the current measured with the current input is slightly more accurate above 100 kHz. Thus, the estimation of the systematic component of the error here is limited to 1% at frequencies up to 500 kHz.

The measured current average is obtained by averaging 40 000 readings over 5 seconds and is further filtered by a 6th order output filter of the lock-in amplifier with a cut-off frequency of 10 Hz. Figures 33 to 37 show the differences between the measured voltage V_{in} and its calculated value when using low ohmic load resistances.

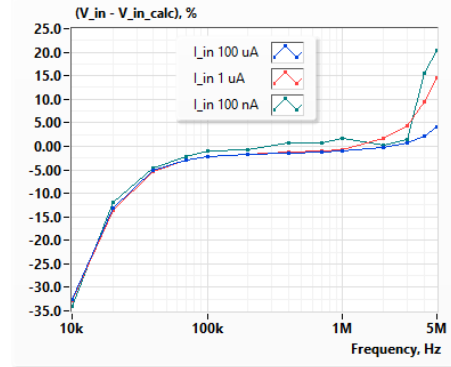
As illustrated in Figure 35, it is not possible for the T50-26 core with 30 turns to have a flat portion of frequency response at a load of 100 Ω . In the case of 10 turns of the same core, this is not possible with both 100 Ω and 10 Ω load, so these dependencies are not shown.

Core ELP18 - PC200, $n_s = 10$, $R_{load} 100 \Omega$



a

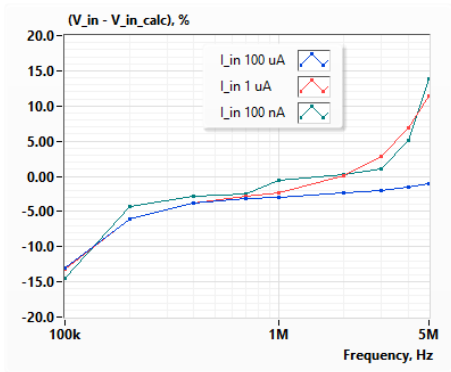
Core ELP18 - PC200, $n_s = 10$, $R_{load} 10 \Omega$



b

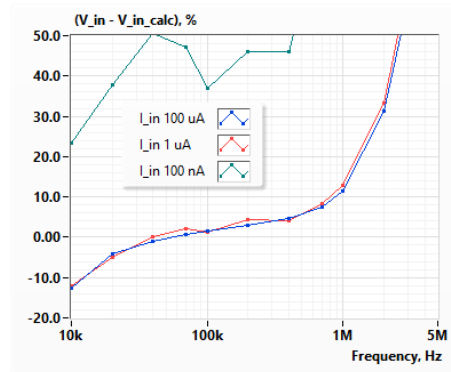
Figure 33. The difference of measured and calculated V_{in} for various measured currents at load resistance 100Ω (a) and 10Ω (b)

T50-26, $n_s = 100$, $R_{load} 100 \Omega$



a

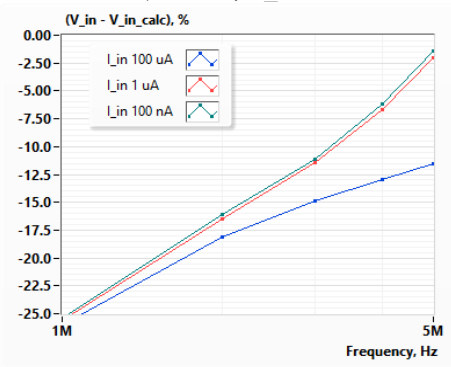
T50-26, $n_s = 100$, $R_{load} 10 \Omega$



b

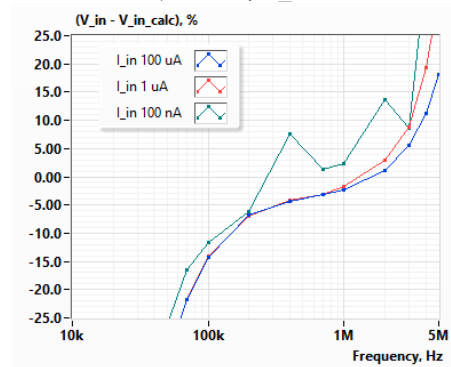
Figure 34. The difference of measured and calculated V_{in} for various measured currents at load resistance 100Ω (a) and 10Ω (b)

T50-26, $n_s = 30$, $R_{load} 100 \Omega$



a

T50-26, $n_s = 30$, $R_{load} 10 \Omega$

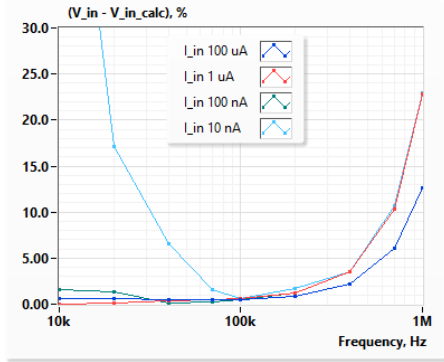


b

Figure 35. The difference of measured and calculated V_{in} for various measured currents at load resistance 100Ω (a) and 10Ω (b)

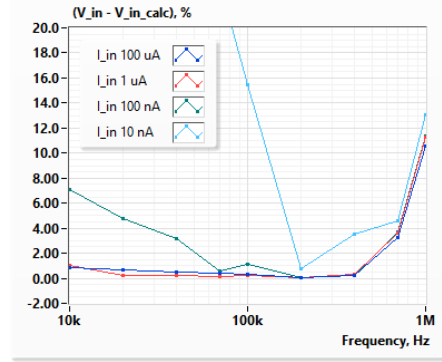
Figures 36 and 37 show the differences between the measured voltage V_{in} and its calculated value when using uniformly increasing portion of the frequency response and $10 \text{ k}\Omega$ load resistance.

Core ELP18 - PC200, $n_s = 10$, $R_{load} 10\text{ k}\Omega$



a

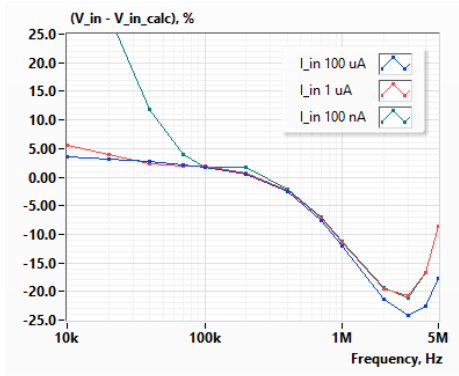
Core T50-26, $n_s = 100$, $R_{load} 10\text{ k}\Omega$



b

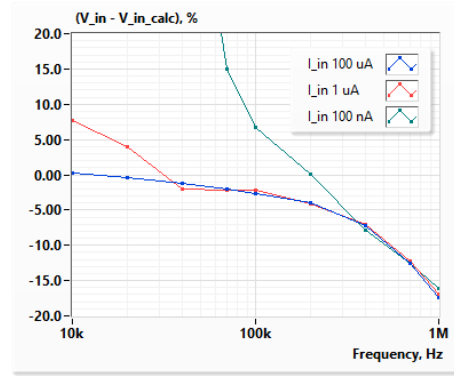
Figure 36. The difference of measured and calculated V_{in} for various measured currents for ELP18 PC200 core with 10 turns (a) and for T50-26 core with 100 turns (b)

Core T50-26, $n_s = 30$, $R_{load} 10\text{ k}\Omega$



a

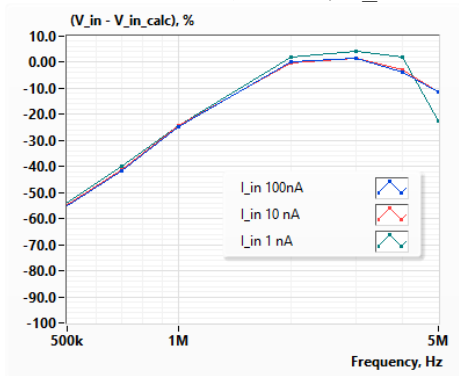
Core T50-26, $n_s = 100$, $R_{load} 10\text{ k}\Omega$



b

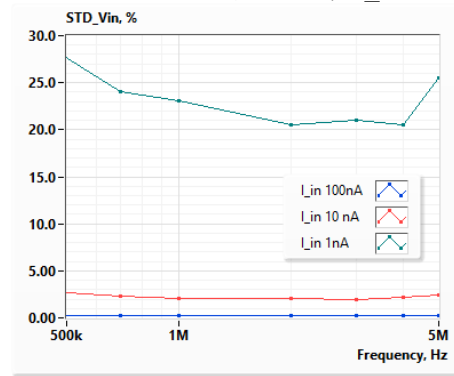
Figure 37. The difference of measured and calculated V_{in} for various measured currents for T50-26 core with 30 turns (a) and 100 turns (b)

Core ELP18 - PC200, $n_s = 10$, $R_{load} 1\text{ k}\Omega$



a

Core ELP18 - PC200, $n_s = 10$, $R_{load} 1\text{ k}\Omega$



b

Figure 38. The difference of measured and calculated V_{in} for the current range from 1 nA to 100 nA (a) and corresponding STD-s (b)

The random component of the error can be estimated from the STD. For a large enough sample, approximately 68% of the readings will be within one standard deviation of the

mean value, 95% of the readings will be in the interval $x \pm 2 \text{ STD}$, and nearly all (99.7%) of readings will lie within three standard deviations from the mean.

4.5 Conclusion based on Measurement results

Experiments have proved that with the used transformers and ZI MFLI lock-in amplifier, it is possible to measure alternating currents from 1 nA to 5 mA (RMS), in the frequency range from 10 kHz to 5 MHz.

Based on the experimental data, it may be concluded that significant systematic and random error components make the measurement results below 100 nA practically useless in the case of using T50-26 core with 10 and 30 turns of the secondary winding. T50-26 core with 100 turns allows measurement of 10 nA current in the frequency range from 100 kHz to 5 MHz, but the random component of measurement error is high with a relative STD near 20%.

The ELP18 core employing higher permeability PC200 ferrite with lower core losses provides almost twice the sensitivity of T50-26 core with 100 turns at only 10 turns. The use of such a solution allows the lower limit of the current measurement in the frequency range 1 MHz to 5 MHz to be increased to 1 nA. However, the accuracy of measurements remains modest in this case, both systematic error, and STD, near 25 % (although a systematic error can be significantly reduced by initial calibration).

The accuracy and resolution of the measurements can be significantly improved by optimizing the number of turns for a narrower frequency range.

In the described setup, there is a noticeable influence of the load on the secondary side of the transformer on the input current. This influence can be hypothetically minimized by active negative feedback using a transformer with two secondary coils. Investigation of this solution is, however, out of the scope of the thesis.

5 Summary and Recommendations

Current measurements are important part of electrical and electronic studies. There are several ways of sensing current such as shunt resistor, Rogowski coil, current transformer, Hall effect and fluxgate sensing. Each of this technique has its limitation. The shunt resistor method is simple; however, it does not provide galvanic isolation and requires electrodes for use in liquids that degrade the accuracy of such measurements. It is complicated to measure small current with Rogowski coil due to its poor sensitivity and susceptibility to external disturbances. Fluxgate sensors have high sensitivity, but its frequency range is limited by the operation principle. Hall effect sensors have modest sensitivity and frequency range. In most typical current transformer, if the winding ratio is high, there will be an increase in parasitic capacitance which reduces the frequency range and common mode noise rejection.

The aim of this thesis is to measure low-level high-frequency current using a transformer, taking note of its sensitivity and accuracy. There are two different types of cores used. These are Amidon's iron powder toroid T50-26 and EPCOS/TDK ELP 18x4x10 ferrite core. These cores have different windings, the series and load resistor are varied for different measurements. The transformer is connected to a MFLI lock-in amplifier which is configured using a LabView for automatic calculation of the result and the display of the graphical representations. The following observations and conclusions have been made:

- The sensitivity of the current measurement increases in proportion to the number of secondary turns as expected.
- ELP18 core employing higher permeability PC200 ferrite with lower core losses provides almost twice the sensitivity of T50-26 core with 100 turns at only 10 turns.
- The sensitivity and accuracy of the measurements can be significantly improved by optimizing the number of turns for a narrower frequency range.

- The current of 1 nA is practically not measurable in a given frequency range when employing T50-26 iron powder toroid cores and $R_{load} \leq 100 \Omega$. However, it is still possible in the frequency range of 1 MHz to 5 MHz when employing higher permeability low-loss PC200 ferrite core and load resistance 1 k Ω .

To further this thesis, I recommend using additional tests to find the optimal number of turns of the secondary winding of the transformer for narrower frequency ranges. Secondly, more accurate determination of measurement errors needs to be considered. To do this, the values of the measured currents must be determined using additional more accurate measuring instruments. In addition, reducing the dimensions of the measuring transformer by using Π -shaped instead of E-shape. This is done for example, by removing one of the outer parts of the E-shape cores. Furthermore, although core losses are described in this thesis, their effects have not been thoroughly analysed. Finally, the experiment should be performed using other core materials.

References

- [1] J. Ojarand, Tutorials “Synchronous Measurement of Low-level High-Frequency Current Using Current Transformer”, Tallinn (Estonia), 2019.
- [2] D. Suitella and J. WINDARTO, “High Precision Fluxgate Current Sensor,” in *ResearchGate Articals*, pp. 1–6, 2011.
- [3] A. C. Kibblewhite and K. C. Ewans, “Wave-wave interactions, microseisms, and infrasonic ambient noise in the ocean,” *J. Acoust. Soc. Am.*, vol. 78, no. 3, pp. 981–994, 1985, doi: 10.1121/1.392931.
- [4] Circuit Globe, “Difference between Electric and Magnetic field,” [WWW] <https://circuitglobe.com/difference-between-electric-and-magnetic-field.html>, March 01, 2020.
- [5] Encyclopedia Britannica, “Electromagnetic field,” [WWW] <https://www.britannica.com/science/electromagnetic-field>, March 03, 2020.
- [6] L. Orozco, “Synchronous Detectors Facilitate Precision, Low-Level Measurements,” *Analog Dialogue*, vol. 48, no. 12, pp. 1-5, 2014.
- [7] Rydh Andreas, “Advantages of synchronized lock-in amplifiers in experiments” (APS March Meeting Abstracts), (<https://ui.adsabs.harvard.edu/abs/2010APS.MARY15012R>), March 2010.
- [8] S. Ziegler, R. C. Woodward, H. H. C. Iu, and L. J. Borle, “Current sensing techniques: A review,” *IEEE Sens. J.*, vol. 9, no. 4, pp. 354–376, 2009, doi: 10.1109/JSEN.2009.2013914.
- [9] Sourav Gupta, “Current Sensing Techniques using Different Current Sensors,” [WWW] <https://circuitdigest.com/article/how-to-measure-current-in-a-circuit-with-different-current-sensing-techniques>, January 04, 2020.
- [10] Hoiki, “6 Current Sensing Methods,” [WWW] <https://hiokiusa.com/6-current-sensing-methods>, January 18, 2020.
- [11] Hoiki, “Current Probes Sensors | Non-contact voltage Probes, CAN sensors Principle of Current Sensors,” [WWW] <https://www.hioki.com/en/products/listUse/?category=17>, October 14, 2019.
- [12] Kapsalis, Vasilis C. (2017). Advances in Magnetic Field Sensors. Journal of Physics: Conference Series. 939. 012026. 10.1088/1742-6596/939/1/012026.
- [13] Texas Instruments, “Six ways to sense current and how to decide which to use,” [WWW] https://e2e.ti.com/blogs_/archives/b/precisionhub/archive/2015/07/10/six-ways-to-sense-current-and-how-to-decide-which-to-use, January 18, 2020.
- [14] G. Velasco-Quesada, M. Roman-Lumbreras, A. Conesa-Roca, and F. Jerez, “Design of a low-consumption fluxgate transducer for high-current measurement applications,” *IEEE Sens. J.*, vol. 11, no. 2, pp. 280–287, 2011, doi: 10.1109/JSEN.2010.2054831.
- [15] M. Laboratories *et al.*, “Transformer Basics Information Guide,” pp. 1–14, 2014.
- [16] Electronics Tutorials, “Transformer Basics,” [WWW] <https://www.electronics-tutorials.ws/transformer/transformer-basics.html>, March 20, 2020.
- [17] Custom Coils, “Theory of operation of a Single-Phase Transformers,” [WWW] <https://www.customcoils.com/theory-of-operation-of-single-phase-transformers>, March

30, 2020.

- [18] Polytechnic Hub, "Difference between Ideal Transformer and Practical Transformer," [WWW] <https://www.polytechnichub.com/difference-between-ideal-and-practical-transformer>, March 18, 2020.
- [19] P. R. Kareem, "TRANSFORMER : Working principle of transformer," *ResearchGate Articals*, May, 2019.
- [20] Goldstone Magnetics, "The Difference Between Ferrite Core and Iron Powder Core," [WWW] <http://www.gsmagnetics.com/news/the-difference-between-ferrite-core-and-iron-p-23212644.html>, March 30, 2020.
- [21] Electric 4 U, "Theory of Inductor," [WWW] <https://www.electrical4u.com/what-is-inductor-and-inductance-theory-of-inductor>, March 19, 2020.
- [22] I. Channel and K. Features, "Lock-in Amplifier Zurich Instrument," 2013.
- [23] Zurich Instruments, "MFLI Lock-in Amplifier," [WWW] <https://www.zhinst.com/americas/products/mfli-lock-amplifier#functional-description>, April 01, 2020.
- [24] Waters, C., "Current Transformers Provide Accurate, Isolated Measurements", *PCIM Magazine*, Dec. 1986.
- [25] Renesas Electronics America Inc. (REA), W. Paper, "Sensing Element for Current Measurement", pp.1-17, 2018.
- [26] Ken Evans MENG CEng MIEE, "Fluxgate Magnetometer Explained", Prestbury (England), March 2006.
- [27] ElectronicWings, "Current Measurement using Current Transformer", [WWW] <https://www.electronicwings.com/users/amrut/projects/current-measurement-using-current-transformer>, January 12, 2020.
- [28] MIT, "Faraday's Law of Induction", [WWW] <https://web.mit.edu/8.02t/www/802TEAL3D/visualizations/coursenotes/modules/guide10.pdf>, October 14, 2019.
- [29] Hayt, W H. 1989. *Engineering Electromagnetics*. Electrical Engineering Series. McGraw-Hill. <https://books.google.ee/books?id=8js-PgAACAAJ>
- [30] M. Arg, "Measurement of high frequency currents with a Rogowski coil," no. June 2014.
- [31] ATO, "Difference Between Current Sensor and Current Transformer", [WWW] <https://www.ato.com/difference-between-current-sensor-and-current-transformer>, November 14, 2019